

University of Windsor

Scholarship at UWindor

Electronic Theses and Dissertations

Theses, Dissertations, and Major Papers

5-17-1969

Analysis of nonorthogonal cable roofs.

T. Kumanan

University of Windsor

Follow this and additional works at: <https://scholar.uwindsor.ca/etd>

Recommended Citation

Kumanan, T., "Analysis of nonorthogonal cable roofs." (1969). *Electronic Theses and Dissertations*. 6570. <https://scholar.uwindsor.ca/etd/6570>

This online database contains the full-text of PhD dissertations and Masters' theses of University of Windsor students from 1954 forward. These documents are made available for personal study and research purposes only, in accordance with the Canadian Copyright Act and the Creative Commons license—CC BY-NC-ND (Attribution, Non-Commercial, No Derivative Works). Under this license, works must always be attributed to the copyright holder (original author), cannot be used for any commercial purposes, and may not be altered. Any other use would require the permission of the copyright holder. Students may inquire about withdrawing their dissertation and/or thesis from this database. For additional inquiries, please contact the repository administrator via email (scholarship@uwindsor.ca) or by telephone at 519-253-3000ext. 3208.

INFORMATION TO USERS

This manuscript has been reproduced from the microfilm master. UMI films the text directly from the original or copy submitted. Thus, some thesis and dissertation copies are in typewriter face, while others may be from any type of computer printer.

The quality of this reproduction is dependent upon the quality of the copy submitted. Broken or indistinct print, colored or poor quality illustrations and photographs, print bleedthrough, substandard margins, and improper alignment can adversely affect reproduction.

In the unlikely event that the author did not send UMI a complete manuscript and there are missing pages, these will be noted. Also, if unauthorized copyright material had to be removed, a note will indicate the deletion.

Oversize materials (e.g., maps, drawings, charts) are reproduced by sectioning the original, beginning at the upper left-hand corner and continuing from left to right in equal sections with small overlaps.

ProQuest Information and Learning
300 North Zeeb Road, Ann Arbor, MI 48106-1346 USA
800-521-0600

UMI[®]

ANALYSIS OF NONORTHOGONAL CABLE ROOFS

A Thesis
Submitted to the Faculty of Graduate Studies in Partial
Fulfillment of the Requirements for the Degree
of Master of Applied Science in Civil
Engineering from the Univer-
sity of Windsor.

by

T.KUMANAN.

Windsor, Ontario, Canada.

May 1969.

UMI Number:EC52753



UMI Microform EC52753
Copyright 2007 by ProQuest Information and Learning Company.
All rights reserved. This microform edition is protected against
unauthorized copying under Title 17, United States Code.

ProQuest Information and Learning Company
789 East Eisenhower Parkway
P.O. Box 1346
Ann Arbor, MI 48106-1346

ABD 9495

Approved:

J. B. Kennedy

G. Abdel-Sayed

W. North

248697

ABSTRACT

Doubly curved cable suspended roofs with two sets of nonorthogonal cables with opposite curvature to form a hyperbolic paraboloid are analyzed both numerically and experimentally. Equations have been presented to determine the initial shape of the unloaded roof and to determine the displacements and tension increments approximately by neglecting the horizontal displacements. The effect of deformation of the frame is also taken into account. Equations have also been derived for more accurate determination of the displacements by taking the horizontal displacements into account. Correction for nonlinearity of the load-deflection behaviour is also applied by an approximate method and by an incremental load method.

A cable roof 240 ft x 120 ft rectangular in plan and with a difference in height of 12 ft between adjacent corners has been analyzed numerically using the two methods mentioned above and the results have been compared. The behaviour of the roof under a uniform load and under concentrated loads at various positions have been determined. The behaviour with change in the pretension in the cables and with change in the degree of nonorthogonality of the cables also has been studied.

To check the validity of the theory, a small scale model was tested and the experimental results have been compared with the theoretically calculated values.

ACKNOWLEDGEMENTS

The author wishes to express his sincere gratitude to Dr. J. B. Kennedy, Professor and Head, Department of Civil Engineering, for his guidance and encouragement throughout this study.

Thanks are also due to: The Canadial International Development Agency for the financial assistance which made this study possible; the staff, Structural Engineering Laboratory of the Department of Civil Engineering for assistance in construction of the model used in the experiment; the staff of the Computer Center at the University of Windsor.

TABLE OF CONTENTS

	Page
ABSTRACT	ii
ACKNOWLEDGEMENTS	iv
LIST OF FIGURES	vi
LIST OF TABLES	xiii
LIST OF PHOTOGRAPHS	ix
LIST OF SYMBOLS	x
Chapter	
1. INTRODUCTION.	1
1.1 About Cable Roofs.	1
1.2 Review of Prior Work.	2
2. DETERMINATION OF THE INITIAL SHAPE OF THE PRESTRESSED UNLOADED ROOF.	5
3. ANALYSIS OF THE LOADED ROOF NEGLECTING HORIZONTAL DISPLACEMENTS.	8
4. ANALYSIS OF THE LOADED ROOF TAKING THE HORIZONTAL DISPLACEMENTS INTO ACCOUNT.	16
5. NUMERICAL STUDIES.	24
5.1 Neglecting Horizontal Displacements.	24
5.2 Taking Horizontal Displacements into Account.	28
6. EXPERIMENTAL STUDY.	42
6.1 Description of Model.	42
6.2 Experimental Procedure.	45
7. DISCUSSION OF RESULTS.	56
8. CONCLUSIONS.	61
APPENDIX A. FLOW CHARTS FOR COMPUTER PROGRAMS.	63
APPENDIX B. LISTING OF A SAMPLE PROGRAM.	68
BIBLIOGRAPHY.	73

LIST OF FIGURES

Figure		Page
2-1	Views of Cable Sections Meeting at a Joint.	4
3-1	Elevation of a Cable Section Before and After Loading.	9
4-1	Forces Acting at a Joint in the Initial and Displaced Positions.	15
4-2	Plan of a Cable Section between Joints i and j.	15
5-1	Views of a 240 ft x 120 ft Hyperbolic Paraboloid Cable Roof.	23
5-2	Plan of the 240 ft x 120 ft Hyperbolic Paraboloid Cable Roof.	27
5-3	Deflection at Joint 1 of the 240 ft x 120 ft Cable Roof under a Uniform Load.	32
5-4	Deflection at Joint 16 of the 240 ft x 120 ft Cable Roof under a Uniform Load.	33
5-5	Deflection at Joint 2 of the 240 ft x 120 ft Cable Roof under a Uniform Load of 1 Kip/joint and a Concentrated Load at Joint 2.	34
5-6	Deflection at Joint 9 of the 240 ft x 120 ft Cable Roof under a Uniform Load of 1 Kip/joint and a Concentrated Load at Joint 9.	35
5-7	Deflection at Joint 16 of the 240 ft x 120 ft Cable Roof under a Uniform Load of 1 Kip/joint and a Concentrated Load at Joint 16.	36
5-8	Deflection at Joint 20 of the 240 ft x 120 ft Cable Roof under a Uniform Load of 1 Kip/joint and a Concentrated Load at Joint 20.	37
5-9	Variation of the Deflection at Joint 1 of the 240 ft x 120 ft Cable Roof with H.	38

Figure		Page
5-10	Variation of the Deflection at Joint 16 of the 240 ft x 120 ft Cable Roof with H.	39
5-10a	Variation of the Tension Increment in the Section of the Cable between Joints 16 and 17 with H.	39a
5-11	Variation of the Deflection at Joint 1 of the 240 ft x 120 ft Cable Roof with R.	40
5-12	Variation of the Deflection at Joint 16 of the 240 ft x 120 ft Cable Roof with R.	41
6-1	Plan of Model.	46
6-2	Deflection at Joint 7 of the Model under a Uniform Load.	47
6-3	Deflection at Joint 9 of the Model under a Uniform Load.	48
6-4	Deflection at Joint 12 of the Model under a Uniform Load.	49
6-5	Deflection at Joint 2 of the Model under a Concentrated Load at Joint 2.	50
6-6	Deflection at Joint 7 of the Model under a Concentrated Load at Joint 7.	51
6-7	Deflection at Joint 8 of the Model under a Concentrated Load at Joint 8.	52
6-8	Deflection at Joint 9 of the Model under a Concentrated Load at Joint 9.	53
6-9	Deflection at Joint 10 of the Model under a Concentrated Load at Joint 10.	54
6-10	Deflection at Joint 11 of the Model under a Concentrated Load at Joint 11.	55

LIST OF TABLES

Table		Page
5-1	Vertical Displacements of the Joints of the 240 ft x 120 ft Cable Roof shown in fig.(5-1).	25
5-2	Tension Increments in the Cables of the 240 ft x 120 ft Cable Roof shown in fig.(5-1).	26
5-3	Vertical and Horizontal Displacements of the Joints of the 240 ft x 120 ft Cable Roof shown in fig.(5-2).	29

LIST OF PHOTOGRAPHS

Photograph	Page
1. Top View of the Unloaded Model.	43
2. A View of the Loaded Model and the Datran Strain Indicating Equipment.	43
3. Top View of the Loaded Model.	44
4. Side View of the Loaded Model.	44

LIST OF SYMBOLS

a	Length in plan, of a cable section between joints.
\underline{A}	Matrix of coefficients of displacements z .
α, β, γ	Angle made by a cable section with the ξ, η , and z axis respectively.
$d\alpha, d\beta, d\gamma$	Increments in the above angles.
d_{ij}	Influence coefficient for deformation of the frame.
\underline{D}	Matrix of influence coefficients.
	Oblique co-ordinates in the horizontal plane.
$d\xi, d\eta$	Displacements in the above directions.
EA	Tensile rigidity of the cable.
f_m	Sag of the cable.
F_m	Actual length of a cable section.
H	Constant horizontal component of tension in the cable.
δH	Increment in the above tension.
H_m, H_n	Horizontal components of tensions in the cables in the ξ and η directions respectively.
i	A joint under consideration.
j	An adjacent joint.
l_m, l_n	Actual length of cables in the ξ and η directions respectively.
$l_{ij}, l_{m,n,n-1}$, etc.	Actual length of a cable section between two joints.
$\delta l_{m,m-1,n}$	
δl_{ij} etc.	Increments in the above lengths.
m, n	Co-ordinates of a joint.

$P_{m,n}$	Load at joint (m,n).
$P_{i\xi}, P_{i\eta},$	
P_{iz}	Loads at joint i in the directions of ξ, η and z axes respectively.
\underline{P}	Matrix of loads.
R	Ratio of the sides of the roof in plan.
T	Tension in the cable.
$T_{m,n,n-1},$	
$T_{n,m,m-1}$	Tensions in a cable section between two joints.
$\delta T_{m,n,n-1}$	
$\delta T_{n,m,m-1}$	Increments in the above tensions.
θ	Angle between the η and y axes.
U_m, U_n	Total movement of the frame in the direction of the cables in the two directions.
\underline{U}	Matrix of frame movements.
V	Vertical component of tension in the cable.
$X_{o,m}, Y_{o,n}$	Length in plan, of cables in the ξ and η directions respectively.
x,y,z	Rectangular co-ordinates axes.
δz	Vertical displacement.
\underline{Z}	Matrix of vertical displacement.

Chapter 1- Introduction.

1.1 About Cable Roofs.

Cable roofs are recently gaining recognition as economical structural forms. This is mainly because they permit very long spans of economical, column-free construction, which suits large exhibition halls, sports stadiums and other similar buildings. The economy of cable roofs is due to the efficiency with which the cable carries the load. The cable carries the load in pure tension and the use of high tensile steel increases its efficiency. The direction of the stresses in the cable roof are expressed by the cables themselves. Another advantage is that, there is no possibility of any buckling of the elements. Prestressing of the cables makes the roof stiff and resistant to uplift due to wind. This permits the use of light materials for covering and also makes it suitable for permanent buildings.

Another reason for the popularity of the cable roof is its aesthetic value. An infinite number of different shapes can be obtained with cable roofs. The different types of cable roofs can be broadly classified into four groups:-

(i) Roofs with a single set of cables with single curvature. Catenary roofs fall into this group. This type of roof is liable to flutter and hence a heavy roof deck will have to be

used.

(ii) Roofs with double set of cables with single curvature. Here the flutter is eliminated due to the damping effect of the secondary cables.

(iii) Roofs with single or double set of cables with double curvature-circular. This is a very economical shape and has the advantage of all the cables being of equal length. This means design of only one cable. The disadvantage of this type is the difficulty of drainage. Drainage outlets will have to be provided at the center of the roof.

(iv) Roofs with a double set of cables with a double curvature-saddle shape. There is no problem of drainage with this type.

One saddle shape which is popular as a roof shape is the rectangular hyperbolic paraboloid with the two sets of cables running diagonally and at right angles to each other. This requires that the roof be a square or a rhombus in plan. When the area to be covered is rectangular, the two sets of cables are nonorthogonal. It is this type of roof that has been analyzed in the present study.

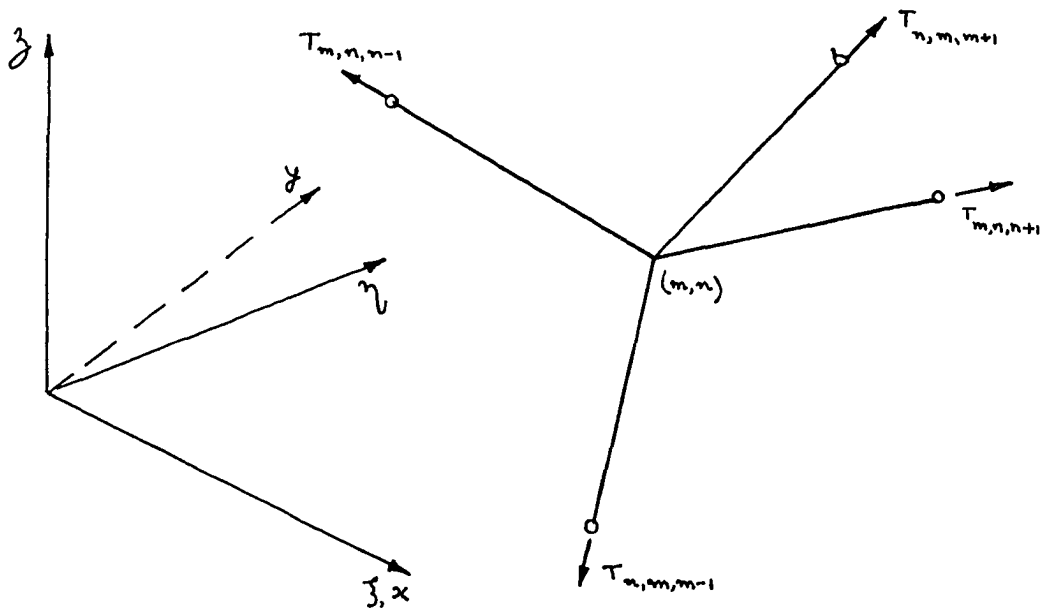
1.2 Review of Prior Work.

In recent years several studies have been published on cable roofs. The book entitled 'Hanging Roofs',¹ the proceedings of a colloquium held by the International Association for Space Structures in Paris on 9-11, July 1962, contains several articles on cable roofs. In a paper presented at this colloquium, a procedure for determining the initial

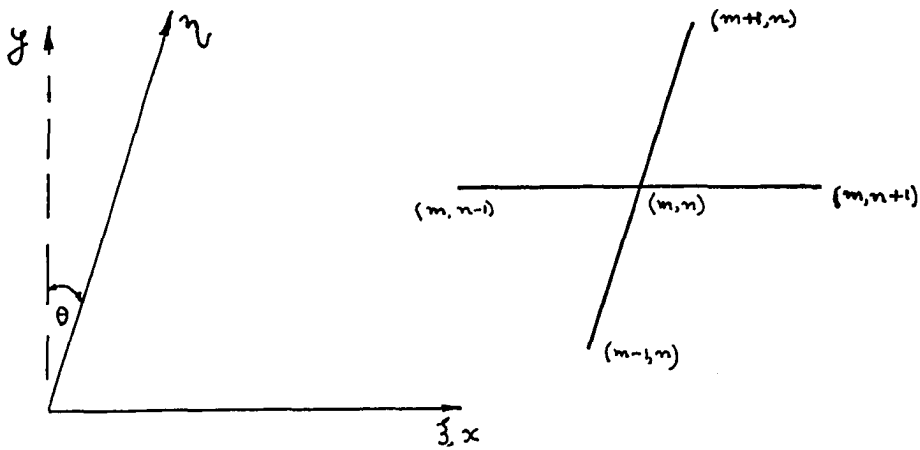
shape of a cable roof was given by Siev³ and Eidelman². They also published a paper which described an approximate method of analysis of prestressed roofs, neglecting the horizontal displacements of the joints. Another paper by Siev⁴ gave a general linear method of analysis with the horizontal displacements taken into account and correction for nonlinearity applied by an iterative procedure. These analyses were for orthogonal nets and assumed the angle between the two sets of cables to be a right angle.

Thornton and Birnstiel⁵ derived nonlinear equations for a three-dimensional suspension structure and used two methods for their solution. An influence coefficient method has been used by Krishna and Sparkes⁶ for the solution of nonlinear equations with the principle of superposition assumed in a limited way to analyze pretensioned cable systems consisting of two cables of reverse curvature, pretensioned together by means of a set of vertical hangers. Buchholdt⁷ used a theory based on the minimization of the total potential energy and a solution by the method of steepest descent. Bathish⁸ used membrane theory to analyze cable roofs. Siev⁹ has analyzed an orthogonal roof bounded by main cables and compared the experimental values.

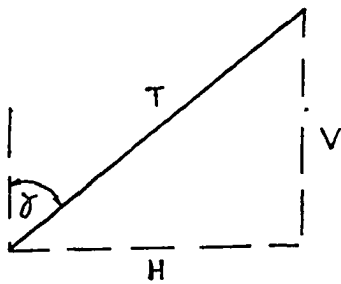
In this study a hyperbolic paraboloid non-orthogonal roof, rectangular in plan, has been analyzed both theoretically and experimentally.



(a) AXONOMETRIC VIEW



(b) PLAN



(c) ELEVATION OF A SINGLE SECTION OF CABLE

Fig.(2-1)- Views of Cable Sections Meeting at a Joint.

Chapter 2- Determination of the Initial Shape of the Prestressed Unloaded Roof.

Considering the equilibrium of a typical joint (m,n), the forces acting at the joint are, the pretension in the cables as shown in fig.(2-1a). The self weight of the cables is neglected for the moment and the net is assumed to be weightless. The self weight could later be considered as part of the external load acting at each joint along with other superimposed loads.

Oblique coordinates ξ and η in the directions of the cables are used for convenience. Resolving forces in the direction of the ξ axis,

$$(H_{m,n,\eta+1} - H_{m,n,\eta-1}) + (H_{n,m,\xi+1} - H_{n,m,\xi-1}) \sin \theta = 0 \quad (2-1)$$

Resolving forces in the direction of the η axis,

$$(H_{n,m,\xi+1} - H_{n,m,\xi-1}) + (H_{m,n,\eta+1} - H_{m,n,\eta-1}) \sin \theta = 0 \quad (2-2)$$

Solving equations (2-1) and (2-2),

$$(H_{m,n,\eta+1} - H_{m,n,\eta-1}) - (H_{n,m,\xi+1} - H_{n,m,\xi-1}) \sin^2 \theta = 0$$

where $H_{m,n,\eta+1}$, $H_{m,n,\eta-1}$ etc. are horizontal components of the tensions in the sections of the cable considered.

$$\text{i.e. } H_{m,n,\eta+1} = H_{m,n,\eta-1} = H_m$$

Similarly,

$$H_{n,m,m+1} = H_{n,m,m-1} = H_n$$

i.e. The horizontal components of the oblique tensile forces are constant throughout the cable.

Resolving in the direction of the z-axis,

$$V_{m,n,n+1} + V_{m,n,n-1} + V_{n,m,m+1} + V_{n,m,m-1} = 0 \quad (2-3)$$

where $V_{m,n,n+1}$, $V_{m,n,n-1}$ etc. are the vertical components of the tensions in the cable sections considered.

From fig.(2-1c),

$$V_{m,n,n+1} = H_m \cot \gamma_{m,n,n+1}$$

where γ is the angle made by the cable section with the vertical.

$$\text{i.e. } V_{m,n,n+1} = H_m \frac{(z_{m,n+1} - z_{m,n})}{a} \quad (2-4a)$$

where a is the length in plan of a cable section and z , the vertical ordinate of the joint.

Similarly,

$$V_{m,n,n-1} = H_m \frac{(z_{m,n-1} - z_{m,n})}{a} \quad (2-4b)$$

$$V_{n,m,m+1} = H_n \frac{(z_{n+1,n} - z_{m,n})}{a} \quad (2-4c)$$

$$V_{n,m,m-1} = H_n \frac{(z_{m-1,n} - z_{m,n})}{a} \quad (2-4d)$$

Substituting equations (2-4) into equation (2-3),

$$H_m (z_{m,n+1} - 2z_{m,n} + z_{m,n-1}) + H_n (z_{m+1,n} - 2z_{m,n} + z_{m-1,n}) = 0 \quad (2-5)$$

If H_m and H_n are arbitrarily fixed, then the ordinates of the joints, z will be the unknowns. The number of unknowns z will be equal to the number of equations (2-5) that can be formulated.

Equation (2-5) can be written in finite difference form as,

$$H_m \left(\frac{\Delta^2 z}{\Delta x^2} \right) + H_n \left(\frac{\Delta^2 z}{\Delta y^2} \right) = 0 \quad (2-6)$$

The ratio H_m/H_n , together with the boundary conditions, determine the exact shape of the roof. It has been shown¹⁰ that for a fixed bounding frame, the variation in the ratio H_m/H_n does not alter the curvature of the roof appreciably in the case of orthogonal nets.

Chapter 3- Analysis of the Loaded Roof Neglecting Horizontal Displacements.

In this chapter, the equations to determine the displacements of the joints and the tension increments in the cables of the roof are derived using an approximate method neglecting horizontal displacements. The horizontal displacements can be expected to be small compared to vertical displacements when the roof is subjected to vertical loads.

Considering the equilibrium of joint (m,n) under a vertical load $P_{m,n}$ acting at the joint, and resolving in the direction of the z -axis,

$$\frac{(H_m + \delta H_m)}{a} \left[(z + \delta z)_{m,n+1} - 2(z + \delta z)_{m,n} + (z + \delta z)_{m,n-1} \right] + \frac{(H_n + \delta H_n)}{a} \left[(z + \delta z)_{m+1,n} - 2(z + \delta z)_{m,n} + (z + \delta z)_{m-1,n} \right] + P_{m,n} = 0 \quad (3-1)$$

where δH is the increase in the horizontal component of tension and δz the vertical displacement.

Subtracting equation (2-5) from equation (3-1) and neglecting second order terms,

$$\frac{H_m}{a} (\delta z_{m,n+1} - 2\delta z_{m,n} + \delta z_{m,n-1}) + \frac{H_n}{a} (\delta z_{m+1,n} - 2\delta z_{m,n} + \delta z_{m-1,n}) + \frac{\delta H_m}{a} (z_{m,n+1} - 2z_{m,n} + z_{m,n-1}) + \frac{\delta H_n}{a} (z_{m+1,n} - 2z_{m,n} + z_{m-1,n}) = -P_{m,n} \quad (3-2)$$

Resolving in the direction of ξ and η axes and neglecting horizontal displacements will result in equations (2-1) and (2-2), which means that the increase in the hori-

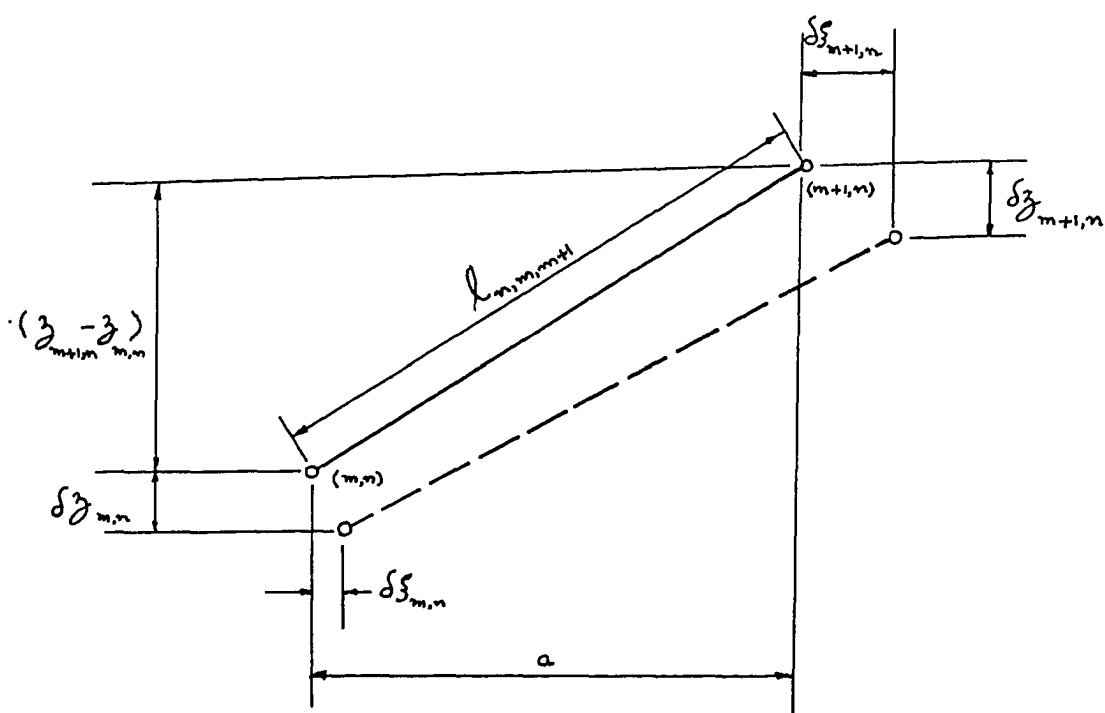


Fig.(3-1)- Elevation of a Cable Section Before and After Loading.

zontal component of the tension is constant throughout the cable.

The elongation of the cable section shown in fig.(3-1) is

$$\delta l_{n,m,m+1} = \frac{\delta T_{n,m,m+1} \cdot l_{n,m,m+1}}{EA_n} \quad (3-3)$$

where δT is the change in tension, $l_{m,m+1,n}$ is the length of the section and EA is the tensile rigidity of the cable.

Also

$$\delta T_{n,m,m+1} = \frac{\delta H_n}{\sin \gamma_{n,m,m+1}} \quad (3-4)$$

and

$$l_{n,m,m+1} = \frac{a}{\sin \gamma_{n,m,m+1}} \quad (3-5)$$

Substituting equations (3-4) and (3-5) in equation (3-3),

$$\begin{aligned} \delta l_{n,m,m+1} &= \frac{\delta H_n}{\sin \gamma_{n,m,m+1}} \cdot \frac{a}{\sin \gamma_{n,m,m+1}} \cdot \frac{1}{EA_n} \\ &= \frac{\delta H_n}{EA_n} \cdot \frac{a}{\sin^2 \gamma_{n,m,m+1}} \end{aligned} \quad (3-6)$$

The elongation of cable n is obtained by summing up the elongations for all such sections of the cable.

$$\text{i.e. } \delta l_n = \frac{a \delta H_n}{EA_n} \sum_m \frac{1}{\sin^2 \gamma_{n,m,m+1}} \quad (3-7)$$

$$\begin{aligned}
 \delta l_n &= \frac{a \cdot \delta H_n}{E A_n} \sum_m \left[1 + \cot^2 \gamma_{n, m, m+1} \right] \\
 &= \frac{a \delta H_n}{E A_n} \sum_m \left[1 + \left(\frac{z_{m+1, n} - z_{m, n}}{a} \right)^2 \right] \\
 &= \frac{\delta H_n}{E A_n \cdot a} \sum_m \left[a^2 + (z_{m+1, n} - z_{m, n})^2 \right] \quad (3-8)
 \end{aligned}$$

Also,

$$\begin{aligned}
 (l_{n, m, m+1} + \delta l_{n, m, m+1})^2 &= (\xi_{m+1, n} + \delta \xi_{m+1, n} - \xi_{m, n} - \delta \xi_{m, n})^2 \\
 &\quad + (z_{m+1, n} + \delta z_{m+1, n} - z_{m, n} - \delta z_{m, n})^2 \quad (3-9)
 \end{aligned}$$

where $\delta \xi$ is the displacement in the ξ direction and

$$l_{n, m, m+1}^2 = (\xi_{m+1, n} - \xi_{m, n})^2 + (z_{m+1, n} - z_{m, n})^2 \quad (3-10)$$

Subtracting equation (3-10) from equation (3-9) and neglecting second order terms,

$$l_{n, m, m+1} \delta l_{n, m, m+1} = a(\delta \xi_{m+1, n} - \delta \xi_{m, n}) + (z_{m+1, n} - z_{m, n})(\delta z_{m+1, n} - \delta z_{m, n})$$

$$\therefore \delta l_n = \sum \left[\frac{1}{l_{n, m+1, m}} \left\{ a(\delta \xi_{m+1, n} - \delta \xi_{m, n}) + (z_{m+1, n} - z_{m, n})(\delta z_{m+1, n} - \delta z_{m, n}) \right\} \right] \quad (3-11)$$

Assuming that the length of two adjacent sections are equal, when the elongations of all sections are summed up, the first term in the bracket represents the distance increment between the two ends of the cable. This is equal to the total movement of the frame at the ends of the

cable and is zero when there is no deformation of the bounding frame.

Considering the inward displacement of the frame to be positive and equal to u ,

$$\delta l_n = \frac{m}{l_n} \left[-u_n a + \sum \{ (z_{m+i,n} - z_{m,n}) (\delta z_{m+i,n} - \delta z_{m,n}) \} \right] \quad (3-12)$$

Equating equations (3-8) and (3-12),

$$\begin{aligned} \delta H_n &= \frac{EA_n a m}{l_n} \frac{[-u_n a + \sum \{ (z_{m+i,n} - z_{m,n}) (\delta z_{m+i,n} - \delta z_{m,n}) \}]}{\sum [a^2 + (z_{m+i,n} - z_{m,n})^2]} \\ &= \frac{EA_n Y_{0,n}}{l_n} \frac{[-u_n a + \sum \{ (z_{m+i,n} - z_{m,n}) (\delta z_{m+i,n} - \delta z_{m,n}) \}]}{\sum [a^2 + (z_{m+i,n} - z_{m,n})^2]} \end{aligned} \quad (3-13a)$$

Similarly,

$$\delta H_m = \frac{EA_m X_{0,m}}{l_m} \frac{[-u_m a + \sum \{ (z_{m,n+i} - z_{m,n}) (\delta z_{m,n+i} - \delta z_{m,n}) \}]}{\sum [a^2 + (z_{m,n+i} - z_{m,n})^2]} \quad (3-13b)$$

Now substituting for δH_m and δH_n in equation

(3-2),

$$\begin{aligned} &\frac{H_m}{a} (\delta z_{m,n+1} - 2\delta z_{m,n} + \delta z_{m,n-1}) + \frac{H_n}{a} (\delta z_{m+1,n} - 2\delta z_{m,n} + \delta z_{m-1,n}) \\ &+ \frac{EA_m X_{0,m}}{a l_m} (z_{m,n+1} - 2z_{m,n} + z_{m,n-1}) \frac{[-u_m a + \sum \{ (z_{m,n+i} - z_{m,n}) (\delta z_{m,n+i} - \delta z_{m,n}) \}]}{\sum [a^2 + (z_{m,n+i} - z_{m,n})^2]} \\ &+ \frac{EA_n Y_{0,n}}{a l_n} (z_{m+1,n} - 2z_{m,n} + z_{m-1,n}) \frac{[-u_n a + \sum \{ (z_{m+i,n} - z_{m,n}) (\delta z_{m+i,n} - \delta z_{m,n}) \}]}{\sum [a^2 + (z_{m+i,n} - z_{m,n})^2]} \\ &= -P_{m,n} \end{aligned} \quad (3-14)$$

where $X_{0,m}$, $Y_{0,n}$ are the length in plan of the cables m and n respectively.

When $H_m = H_n = H$, equation (3-14) may be written

$$\begin{aligned}
 & H(\delta z_{m,n+1} + \delta z_{m,n-1} + \delta z_{m+1,n} + \delta z_{m-1,n} - 4\delta z_{m,n}) \\
 & + \frac{EA_m X_{0,m}}{l_m} (z_{m,n+1} - 2z_{m,n} + z_{m,n-1}) \frac{[-U_m a + \sum \{(z_{m,n+1} - z_{m,n})(\delta z_{m,n+1} - \delta z_{m,n})\}]}{\sum [a^2 + (z_{m,n+1} - z_{m,n})^2]} \\
 & + \frac{EA_n Y_{0,n}}{l_n} (z_{m+1,n} - 2z_{m,n} + z_{m-1,n}) \frac{[-U_n a + \sum \{(z_{m+1,n} - z_{m,n})(\delta z_{m+1,n} - \delta z_{m,n})\}]}{\sum [a^2 + (z_{m+1,n} - z_{m,n})^2]} \\
 & = a \cdot P_{m,n} \quad (3-15)
 \end{aligned}$$

The number of equations (3-15) that can be written is equal to the number of joints and when the frame deformations U_m , U_n are zero, is equal to the number of unknowns δz .

Equation (3-15) can be written in the matrix form as

$$\underline{A} \underline{Z} = \underline{P} \quad (3-16)$$

or

$$\underline{Z} = \underline{A}^{-1} \underline{P}$$

When the frame deformation is to be taken into account, the number of unknowns is in excess of the number of equations by the total number of cables. To calculate the effect of frame deformation, the horizontal inward displacements of the frame between the two anchorage points of each cable is determined. Hence the influence coefficients for the deformation of the frame are obtained.

Thus

$$\begin{Bmatrix} u_1 \\ \vdots \\ u_{m+n} \end{Bmatrix} = \begin{bmatrix} d_{11} & \dots & d_{1,m+n} \\ \vdots & \ddots & \vdots \\ d_{m+n,1} & \dots & d_{m+n,m+n} \end{bmatrix} \begin{Bmatrix} \delta H_1 \\ \vdots \\ \delta H_{m+n} \end{Bmatrix}$$

where d_{11} etc. are the influence coefficients ,

or

$$\underline{U} = \underline{D} \cdot \underline{\Delta H} \quad (3-17)$$

Equations (3-17) can be substituted into equations (3-13) and (3-14) which can be solved to obtain the displacements δz and the horizontal components of the tension increments δH directly.

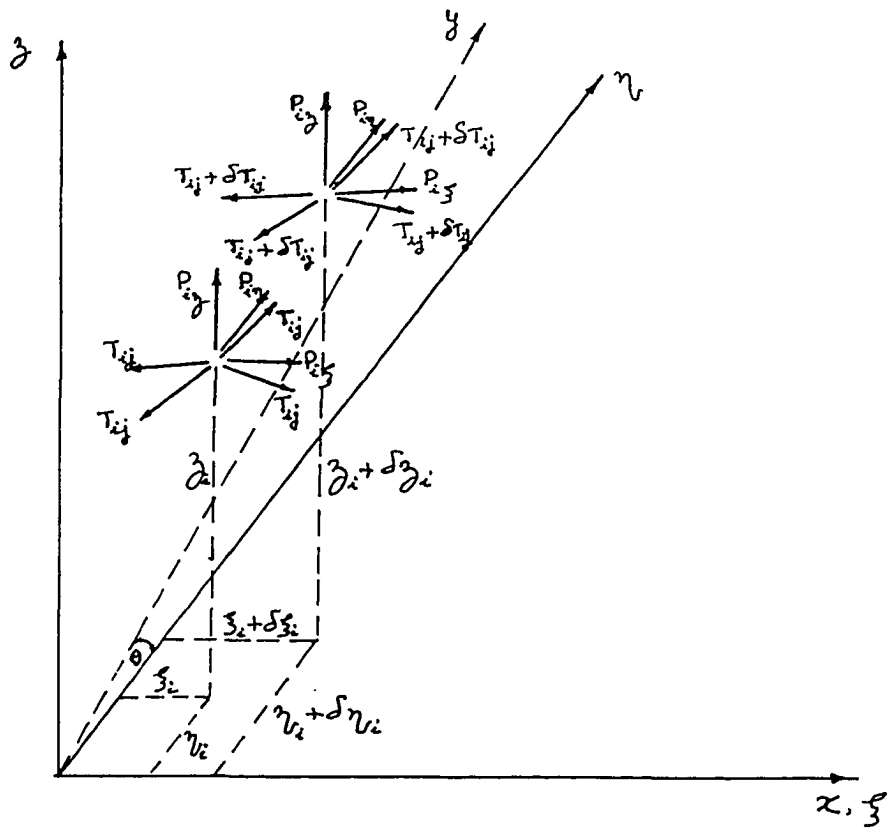


Fig.(4-1)- Forces acting at a Joint in the Initial and Displaced Positions.

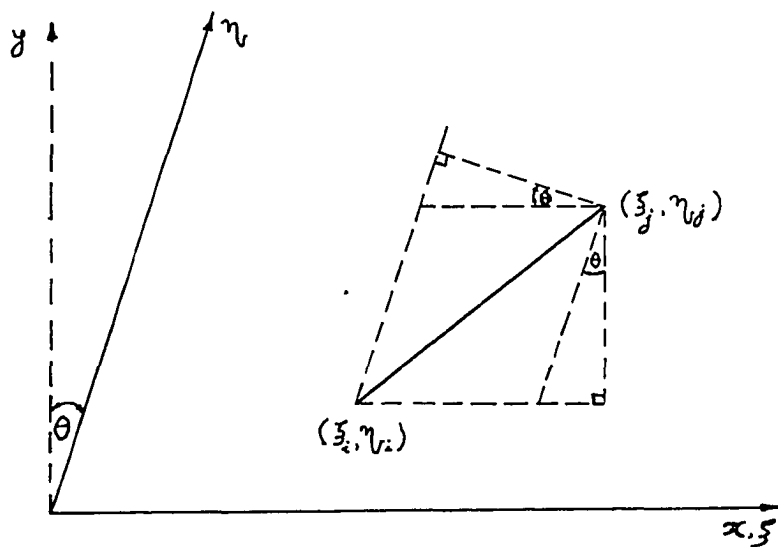


Fig.(4-2)- Plan of a Cable Section between Joints i and j.

Chapter 4- Analysis of the Loaded Roof Taking the Horizontal Displacements into Account.

Resolving the forces at a joint i [fig.(4-1)] in all three directions, viz. ξ, η and z directions,

$$\sum \{ (T_{ij} + \delta T_{ij}) \cos (\alpha + \delta \alpha)_{ij} \} + P_{i\xi} = 0 \quad (4-1a)$$

$$\sum \{ (T_{ij} + \delta T_{ij}) \cos (\beta + \delta \beta)_{ij} \} + P_{i\eta} = 0 \quad (4-1b)$$

$$\sum \{ (T_{ij} + \delta T_{ij}) \cos (\gamma + \delta \gamma)_{ij} \} + P_{iz} = 0 \quad (4-1c)$$

where α, β, γ are the angles made by a cable section with the ξ, η and z axes respectively.

The extended length of the cable section between joints i and j is given by,

$$\begin{aligned} (l_{ij} + \delta l_{ij})^2 = & (x_i + \delta x_i - x_j - \delta x_j)^2 + (y_i + \delta y_i - y_j - \delta y_j)^2 \\ & + (z_i + \delta z_i - z_j - \delta z_j)^2 \end{aligned} \quad (4-2a)$$

and the original length is given by,

$$l_{ij}^2 = (x_i - x_j)^2 + (y_i - y_j)^2 + (z_i - z_j)^2 \quad (4-2b)$$

Subtracting equation (4-2b) from equation (4-2a) and neglecting second order terms,

$$\begin{aligned} l_{ij} \delta l_{ij} = & (x_i - x_j)(\delta x_i - \delta x_j) + (y_i - y_j)(\delta y_i - \delta y_j) \\ & + (z_i - z_j)(\delta z_i - \delta z_j) \end{aligned} \quad (4-3)$$

Now,

$$x = \xi + \eta \sin \theta$$

$$y = \eta \cos \theta$$

where θ is the angle between the η and y axes.

$$\therefore \delta x = \delta \xi + \delta \eta \sin \theta$$

$$\delta y = \delta \eta \cos \theta$$

where $\delta \xi$ and $\delta \eta$ are displacements in the direction of ξ and η axes respectively.

Also from fig.(4-2),

$$\cos \alpha_{ij} = \frac{(\xi_j - \xi_i) + (\eta_j - \eta_i) \sin \theta}{l_{ij}}$$

$$\cos \beta_{ij} = \frac{(\eta_j - \eta_i) + (\xi_j - \xi_i) \sin \theta}{l_{ij}}$$

$$\cos \gamma_{ij} = \frac{(\xi_j - \xi_i)}{l_{ij}}$$

$$\therefore \cos(\alpha + \delta \alpha)_{ij} = \frac{\cos \alpha_{ij} + \frac{(\delta \xi_j - \delta \xi_i) + (\delta \eta_j - \delta \eta_i) \sin \theta}{l_{ij}}}{1 + \frac{\delta l_{ij}}{l_{ij}}}$$

where $\delta \alpha$ is the increment in the angle α .

$$\text{i.e. } \cos(\alpha + \delta \alpha)_{ij} = \left[\cos \alpha_{ij} + \frac{(\delta \xi_j - \delta \xi_i) + (\delta \eta_j - \delta \eta_i) \sin \theta}{l_{ij}} \right] \left(1 - \frac{\delta l_{ij}}{l_{ij}} \right)$$

since $\frac{\delta l_{ij}}{l_{ij}}$ is small.

$$\text{i.e. } \cos(\alpha + \delta \alpha)_{ij} = \left(1 - \frac{\delta l_{ij}}{l_{ij}} \right) \cos \alpha_{ij} + \frac{(\delta \xi_j - \delta \xi_i) + (\delta \eta_j - \delta \eta_i) \sin \theta}{l_{ij}} \quad (4-4a)$$

neglecting second order terms.

Similarly,

$$\cos(\beta + \delta\beta)_{ij} = \cos\beta_{ij} \left(1 - \frac{\delta l_{ij}}{l_{ij}}\right) + \frac{(\delta\eta_{ij} - \delta\eta_i) + (\delta\xi_i - \delta\xi_i) \sin\theta}{l_{ij}} \quad (4-4b)$$

$$\cos(\gamma + \delta\gamma)_{ij} = \cos\gamma_{ij} \left(1 - \frac{\delta l_{ij}}{l_{ij}}\right) + \frac{(\delta z_i - \delta z_i)}{l_{ij}} \quad (4-4c)$$

Substituting now in equation (4-3) for x, y, δx and δy ,

$$l_{ij} \delta l_{ij} = (\xi_i + \eta_{ij} \sin\theta - \xi_i - \eta_i \sin\theta) (\delta\xi_i + \delta\eta_{ij} \sin\theta - \delta\xi_i - \delta\eta_i \sin\theta) \\ + (\eta_{ij} - \eta_i) (\delta\eta_{ij} - \delta\eta_i) \cos^2\theta + (z_i - z_i) (\delta z_i - \delta z_i)$$

$$\text{i.e. } \delta l_{ij} = (\delta\xi_i - \delta\xi_i + \delta\eta_{ij} - \delta\eta_i \sin\theta) \cos\alpha_{ij} \\ + (\delta\eta_{ij} - \delta\eta_i) (\cos\beta_{ij} - \sin\theta \cos\alpha_{ij}) + (\delta z_i - \delta z_i) \cos\gamma_{ij}$$

$$\text{i.e. } \delta l_{ij} = (\delta\xi_i - \delta\xi_i) \cos\alpha_{ij} + (\delta\eta_{ij} - \delta\eta_i) \cos\beta_{ij} + (\delta z_i - \delta z_i) \cos\gamma_{ij} \quad (4-5)$$

Also,

$$\delta l_{ij} = \frac{\delta T_{ij} l_{ij}}{EA} \quad (4-6)$$

Combining this with equation (4-5),

$$\frac{\delta T_{ij} l_{ij}}{EA} = (\delta\xi_i - \delta\xi_i) \cos\alpha_{ij} + (\delta\eta_{ij} - \delta\eta_i) \cos\beta_{ij} + (\delta z_i - \delta z_i) \cos\gamma_{ij} \quad (4-7)$$

Now considering equations (4-1), the corresponding equations before loading,

$$\sum (T_{ij} \cos \alpha_{ij}) = 0 \quad (4-8a)$$

$$\sum (T_{ij} \cos \beta_{ij}) = 0 \quad (4-8b)$$

$$\sum (T_{ij} \cos \gamma_{ij}) = 0 \quad (4-8c)$$

Subtracting equation (4-8a) from equation (4-1a) and omitting terms of second order,

$$\sum [T_{ij} (\cos(\alpha + \delta\alpha)_{ij} - \cos \alpha_{ij}) + \delta T_{ij} \cos \alpha_{ij}] + P_i \delta = 0$$

Substituting from equation (4-4a)

$$\sum [T_{ij} \left\{ \frac{(\delta \xi_i - \delta \xi_j) + (\delta \eta_i - \delta \eta_j) \sin \theta}{l_{ij}} - \frac{\delta l_{ij} \cos \alpha_{ij}}{l_{ij}} \right\} + P_i \delta] = 0$$

Substituting again for δl_{ij} from equation (4-6)

$$\sum [T_{ij} \left\{ \frac{(\delta \xi_i - \delta \xi_j) + (\delta \eta_i - \delta \eta_j) \sin \theta}{l_{ij}} - \frac{\delta T_{ij}}{EA} \cos \alpha_{ij} \right\} + \delta T_{ij} \cos \alpha_{ij}] + P_i \delta = 0$$

Substituting now for δT_{ij} from equation (4-7)

$$\begin{aligned} \sum [& \frac{T_{ij}}{l_{ij}} \{ (\delta \xi_i - \delta \xi_j) + (\delta \eta_i - \delta \eta_j) \sin \theta \\ & + (1 - \frac{T_{ij}}{EA}) \frac{EA}{l_{ij}} \cos \alpha_{ij} \{ (\delta \xi_i - \delta \xi_j) \cos \alpha_{ij} + (\delta \eta_i - \delta \eta_j) \cos \beta_{ij} \\ & + (\delta \gamma_i - \delta \gamma_j) \cos \gamma_{ij} \}] + P_i \delta = 0 \end{aligned}$$

Assuming that the length of two adjacent sections are equal,

$$\frac{a}{l_{ij}} = \frac{x_{o,m}}{l_m} = \frac{1}{1 + \frac{8}{3} \frac{b_m^2}{x_{o,m}^2}}$$

for a flat parabola.

It is also convenient to use the horizontal component H of the initial tension, which is constant throughout the cable instead of T_{ij} which varies from section to section.

$$\text{i.e.} \quad T_{ij} \sin \gamma_{ij} = H$$

or

$$T_{ij} = H / \sin \gamma_{ij}$$

Also replacing $a \left(1 + \frac{8}{3} \frac{b_m^2}{x_{o,m}^2} \right)$ by F_m and

rearranging terms,

$$\begin{aligned} & \sum \left[(\delta x_j - \delta x_i) \left\{ \frac{H \sin^2 \alpha_{ij}}{F_m \sin \gamma_{ij}} + \frac{EA \cos^2 \alpha_{ij}}{F_m} \right\} \right. \\ & + (\delta y_j - \delta y_i) \left\{ \frac{H \sin \theta}{F_m \sin \gamma_{ij}} + \left(EA - \frac{H}{\sin \gamma_{ij}} \right) \frac{\cos \alpha_{ij} \cos \beta_{ij}}{F_m} \right. \\ & \left. \left. + (\delta z_i - \delta z_j) \left(EA - \frac{H}{\sin \gamma_{ij}} \right) \frac{\cos \alpha_{ij} \cos \gamma_{ij}}{F_m} \right] + P_{i3} = 0 \quad (4-9a) \end{aligned}$$

Similarly,

$$\begin{aligned} & \sum \left[(\delta \xi_i - \delta \xi_j) \left\{ \frac{H \sin \theta}{F_m \sin \gamma_{ij}} + \left(EA - \frac{H}{\sin \gamma_{ij}} \right) \frac{\cos \alpha_{ij} \cos \beta_{ij}}{F_m} \right\} \right. \\ & + (\delta \eta_i - \delta \eta_j) \left\{ \frac{H \sin^2 \beta_{ij}}{F_m \sin \gamma_{ij}} + \frac{EA \cos^2 \beta_{ij}}{F_m} \right\} \\ & \left. + (\delta z_i - \delta z_j) \left(EA - \frac{H}{\sin \gamma_{ij}} \right) \frac{\cos \beta_{ij} \cos \gamma_{ij}}{F_m} \right] + P_{i\eta} = 0 \quad (4-9b) \end{aligned}$$

$$\begin{aligned} & \sum \left[(\delta \xi_i - \delta \xi_j) \left(EA - \frac{H}{\sin \gamma_{ij}} \right) \frac{\cos \alpha_{ij} \cos \gamma_{ij}}{F_m} \right. \\ & + (\delta \eta_i - \delta \eta_j) \left(EA - \frac{H}{\sin \gamma_{ij}} \right) \frac{\cos \beta_{ij} \cos \gamma_{ij}}{F_m} \\ & \left. + (\delta z_i - \delta z_j) \left\{ \frac{H \sin \gamma_{ij}}{F_m} + \frac{EA \cos^2 \gamma_{ij}}{F_m} \right\} \right] + P_{iz} = 0 \quad (4-9a) \end{aligned}$$

Correction for Nonlinearity

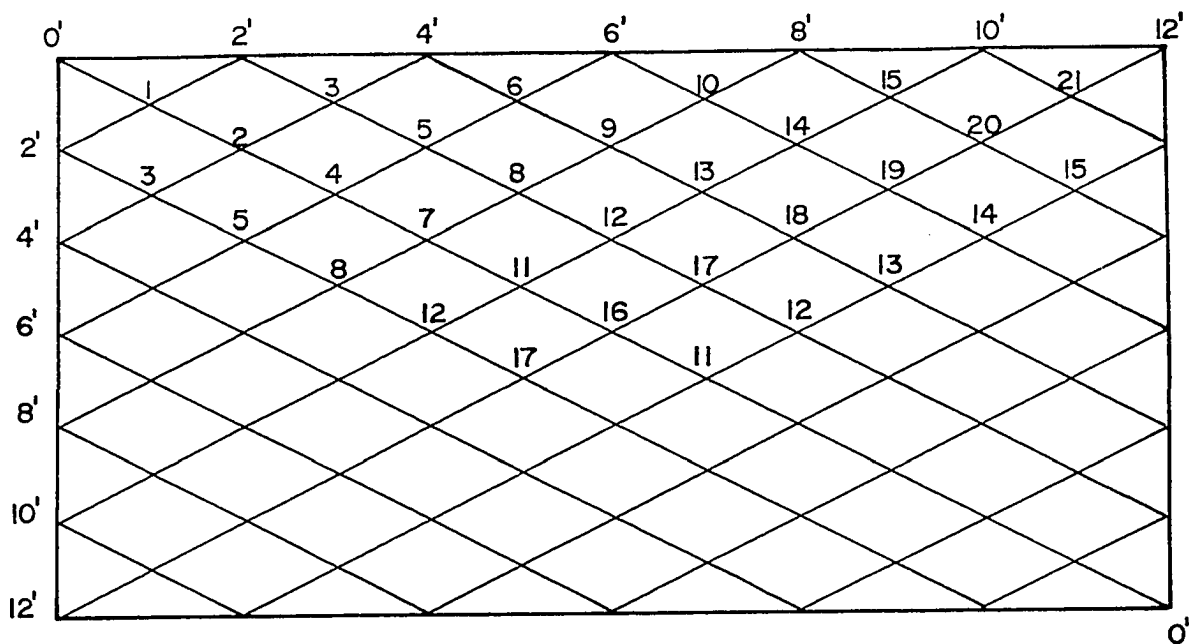
In deriving the above equations, the higher order terms were neglected as being small. This is true only for an infinitesimal load. For larger loads, the behaviour is nonlinear and the correction for this is applied in two ways: (i) by an approximate method (ii) by an incremental load method.

(i) Approximate Method of Correction.

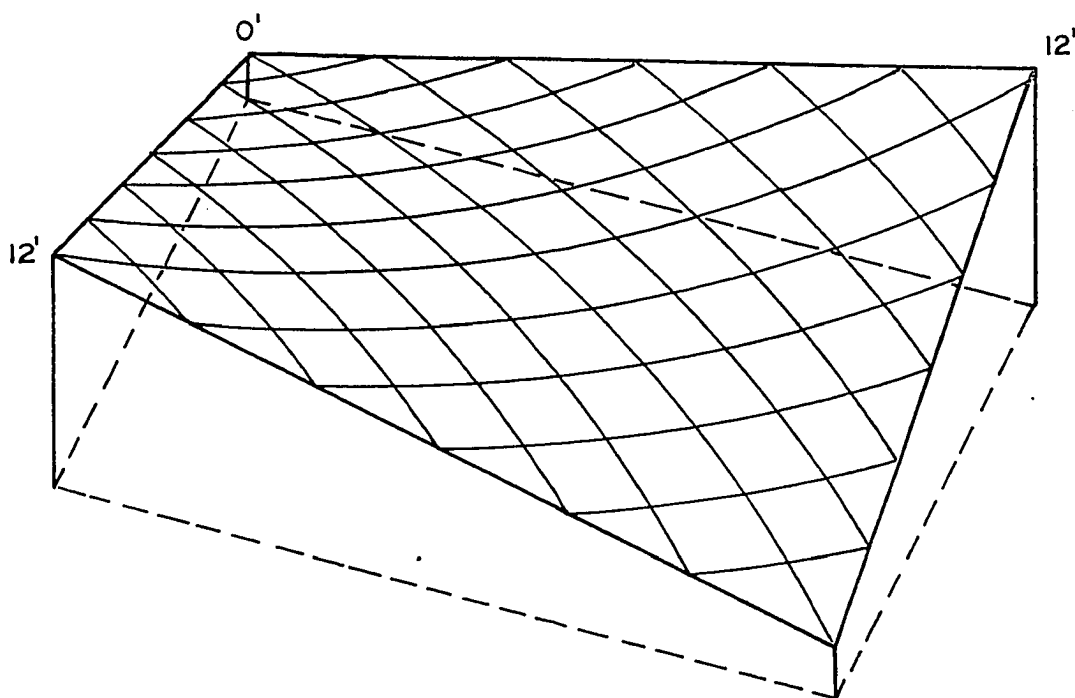
In this method, half the displacements obtained by solving equations (4-9) are added to the initial co-ordinates and the new displacements are calculated using the corrected co-ordinates. The iteration is continued until the values converge sufficiently. This correction amounts to basing the calculations on a configuration which is half-way between the initial and the final (displaced) configurations.

(ii) Incremental Load Method.

Here, the load is applied in small increments and the calculations are based on the previous displaced configuration. The accuracy of the final displacement depends on the size of the increment; the smaller the increment, the greater is the accuracy.



(a) PLAN



(b) AXONOMETRIC VIEW

Fig. (5-1)- Views of a 240 ftx 120 ft Hyperbolic Paraboloid Cable Roof.

Chapter 5- Numerical Studies.

5.1 Neglecting Horizontal Displacements.

A hyperbolic paraboloid roof 240 ft x 120 ft rising by 12 ft from two opposite corners to the two adjacent corners shown in fig.(5-1), was analyzed by using the method mentioned in chapter 2, neglecting frame deformation. The ordinates of the joints were first determined by solving equations (2-5) for the roof. Equations (3-16) were then formulated for the loaded roof and were solved to obtain the resultant displacements. The calculations were done for one quarter of the net consisting of 21 joints for equal loads at all joints and a tension of 50 Kips in all the cables. With the deformation of the frame neglected the number of equations that had to be solved was twenty one.

The same roof was analyzed using equations (3-16) taking the deformation of the frame into account. For this purpose, the frame was assumed to consist of four beams simply supported at their ends. The flexural rigidity of the beams were taken as $96,000 \text{ Kip-in}^2$. The number of equations in this case was thirty three; twenty one for the joints and six for cables in each direction, the others being determined by symmetry. In both cases the equations were solved on the IBM S/360 computer using the available subroutine. The results of the calculations are shown in tables (5-1) and (5-2).

Table (5-1)- Vertical Displacements of the Joints of
240 ft x 120 ft Roof shown in fig.(5-1).

$$H = 50 \text{ Kips, } EA = 30 \times 10^3 \text{ Kip}$$

Joint No.	Vertical Displacements (ft)			
	Load = 1 Kip/joint		Load = 1 Kip/joint 5 Kips at joint 16	
	Without frame de- formation	With frame de- formation	Without frame de- formation	With frame de- formation
1	.218095	.199978	.215975	.194460
2	.543592	.535913	.559846	.550742
3	.398608	.397683	.411660	.410576
4	.860394	.874873	.927712	.944904
5	.755987	.773634	.810777	.831731
6	.461982	.475346	.490521	.506381
7	1.115842	1.149762	1.289348	1.329612
8	1.036608	1.072337	1.169473	1.211885
9	.813359	.842227	.888684	.922938
10	.461982	.475346	.490521	.506381
11	1.281914	1.324941	1.678529	1.729610
12	1.217212	1.261412	1.473241	1.525713
13	1.036608	1.072338	1.169473	1.211886
14	.755987	.773635	.810777	.831732
15	.398608	.397684	.411661	.410577
16	1.341772	1.383839	2.284966	2.334901
17	1.281914	1.324942	1.678529	1.729661
18	1.115842	1.149763	1.289348	1.329613

248697

Table (5-1) (contd.)

Joint No.	Vertical Displacements (ft)			
	Load = 1 Kip/joint		Load = 1 Kip/joint 5 Kips at joint 16	
	Without frame de- formation	With frame de- formation	Without frame de- formation	With frame de- formation
19	.860394	.874874	.927712	.944906
20	.543592	.535914	.559846	.550744
21	.218095	.199977	.215975	.194460

Table (5-2)- Tension Increments in the Cables of
240 ft x 120 ft Roof shown in fig.(5-1).

$$H = 50 \text{ Kips, } EA = 30 \times 10^3 \text{ Kip}$$

Cable	Tension Increments			
	Load = 1 Kip/joint		Load = 1 Kip/joint 5 Kips at joint 16	
	Without frame de- formation	With frame de- formation	Without frame de- formation	With frame de- formation
A	2.180143	11.610423	2.158948	13.359888
B	6.698583	10.194946	6.910206	11.056641
C	10.973134	11.227890	11.752017	12.054489
D	14.321753	13.025525	15.936039	14.399319
E	16.155577	14.709006	18.768974	17.050598
F	15.583756	15.871707	19.315206	19.657135

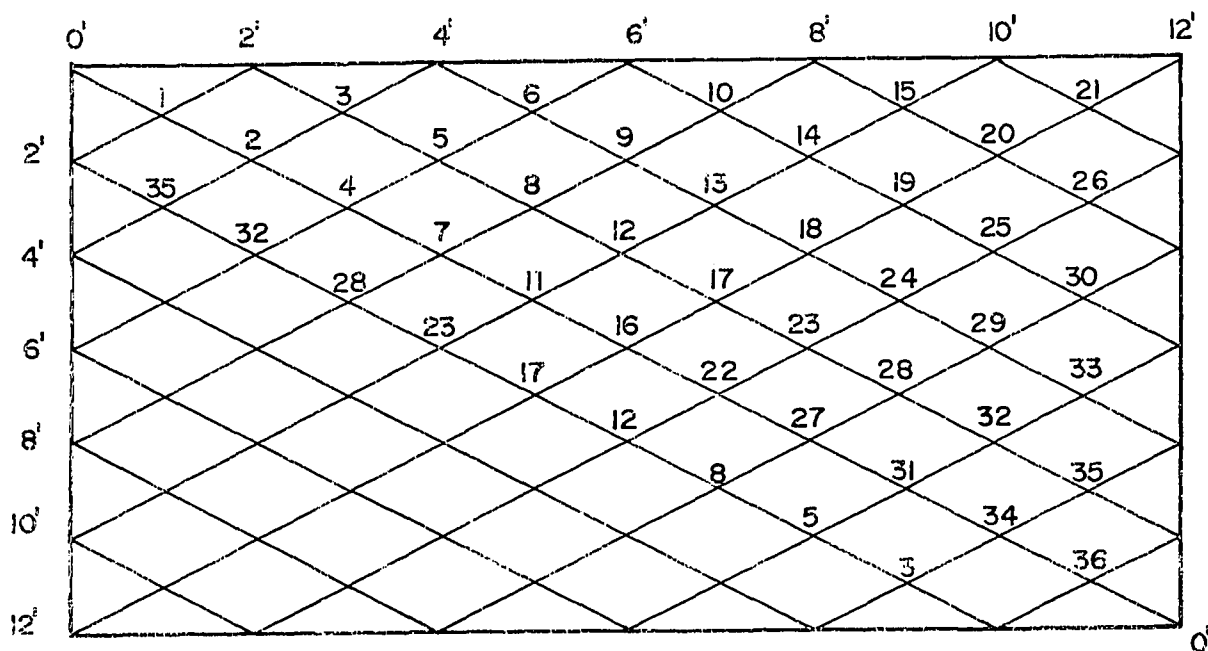


Fig.(5-2)- Plan of the 240. ft x 120 ft Hyperbolic Paraboloid Cable Roof.

5.2 Taking Horizontal Displacements into Account.

The roof referred to in (5.1) was analyzed using the general theory given in chapter 4. In this case, half the net was used for calculations since there is no symmetry within half the net. There is only antisymmetry about the diagonals. For example, for a joint like joint 3, fig.(5-2) there is a corresponding joint in the opposite corner in the other half of the net which has the same vertical displacement but equal and opposite horizontal displacements as joint 3. Equations (4-9) were written for the joints. A program was written for the IBM S/360 computer to form the 108 x 108 matrix, solve the equations using the available subroutine to obtain the displacements, modify the co-ordinates and recalculate the displacements until a satisfactory convergence was reached. The tension increment in each section of the cable was then calculated using the final displacements. The program was also modified for the incremental load method for comparison of the results. Flow charts for the two programs and the computer program for the incremental load method are shown in the appendix.

The calculations were performed for various loadings and varying parameters:-

- (i) Equal loads at all joints with H , the horizontal component of tension fixed at 50 Kips in all the cables. The loads were increased by equal increments and the nonlinear variation of the deflections obtained. Typical results are shown in table (5-3) and the behaviour of joints

Table (5-3)- Vertical and Horizontal Displacements of the
Joints of 240 ft x 120 ft Roof shown in fig.(5-2).

H = 50 Kips, EA = 30×10^3 Kip, Load = 1 Kip/joint

Joint No.	Horizontal Displacements (ft)		Vertical Displacements (ft)
	ξ direction	η direction	
1	.009043	-.005419	-0.205983
2	.022490	-.013440	-0.518198
3	.014274	-.003338	-0.382553
4	.028636	-.017070	-0.829292
5	.018983	-.002147	-0.732224
6	.005984	.007660	-0.450873
7	.025604	-.015218	-1.088215
8	.014322	.003442	-1.014998
9	.001917	.017658	-0.801635
10	-.004715	.018791	-0.458200
11	.014965	-.008864	-1.262860
12	.002812	.011588	-1.203370
13	-.008426	.027513	-1.031159
14	-.014310	.032873	-0.756990
15	-.011860	.023797	-0.401313
16	.000000	.000000	-1.328606
17	-.011429	.019288	-1.273480
18	-.019673	.033057	-1.115296
19	-.021873	.036605	-0.866189
20	-.016670	.027870	-0.551684

Table (5-3) (contd.)

Joint No.	Horizontal Displacements (ft)		Vertical Displacements (ft)
	ξ direction	η direction	
21	-.006113	.010200	-0.224608
22	-.014965	.008864	-1.262858
23	-.027037	.029266	-1.202629
24	-.032969	.042011	-1.029952
25	-.030697	.042509	-0.755783
26	-.019162	.028061	-0.400632
27	-.025605	.015217	-1.088214
28	-.036182	.033449	-1.013703
29	-.036475	.040412	-0.799682
30	-.024782	.030633	-0.456666
31	-.028634	.017069	-0.829292
32	-.035728	.030449	-0.730763
33	-.026599	.027022	-0.449147
34	-.022491	.013440	-0.518198
35	-.023728	.019355	-0.381486
36	-.009043	.005419	-0.205985

1 and 16 are shown in figs.(5-3) and (5-4) respectively.

(ii) Equal loads at all joints and in addition a concentrated load at one of the joints under the same conditions as in (i). The concentrated load was placed at various joints and the calculations were repeated. The behaviour of

the different joints are shown in figs. (5-5) to (5-8).

(iii) The pretension in the cables was varied and the calculations performed for a symmetrical loading of 1 Kip/joint and an unsymmetrical loading of 1 Kip/joint in addition to a concentrated load of 5 Kips at joint 2. The behaviour of joints 1 and 16 with the change in pretension is shown in figs. (5-9) and (5-10).

(iv) The ratio of the sides of the rectangle was varied keeping the smaller side equal to 120 ft and H equal to 50 Kips. This varies the obliquity of the angle between the two sets of cables. The variation was from r , the ratio of the sides of the rectangle = 1 which is an orthogonal net with $\sin \theta = 0$, to $r = 2$ for a net with $\sin \theta = 3/5$. Here too the calculations were done for the two loadings mentioned in (iii). The behaviour of joints 1 and 16 with the variation in the degree of nonorthogonality is shown in figs. (5-11) and (5-12).

In all these cases, the approximate method of correction for nonlinearity was used. In case (i) and case (ii), the calculations were repeated with the incremental load method for comparison.

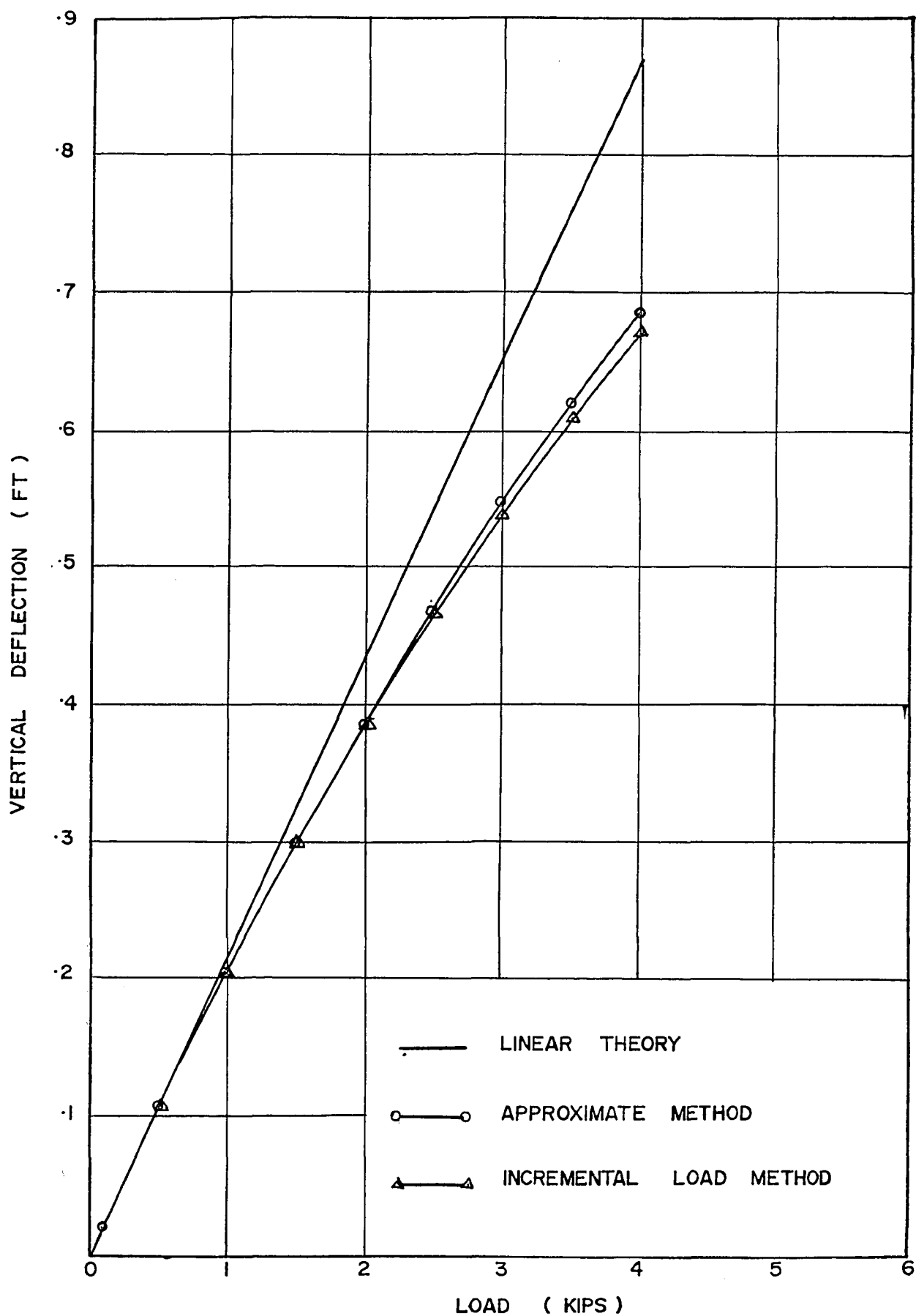


Fig.(5-3)- Deflection at Joint 1 of the 240 ft x 120 ft
Cable Roof under a Uniform Load. ($H=50$ Kips, $EA=30 \times 10^3$ Kip)
-32-

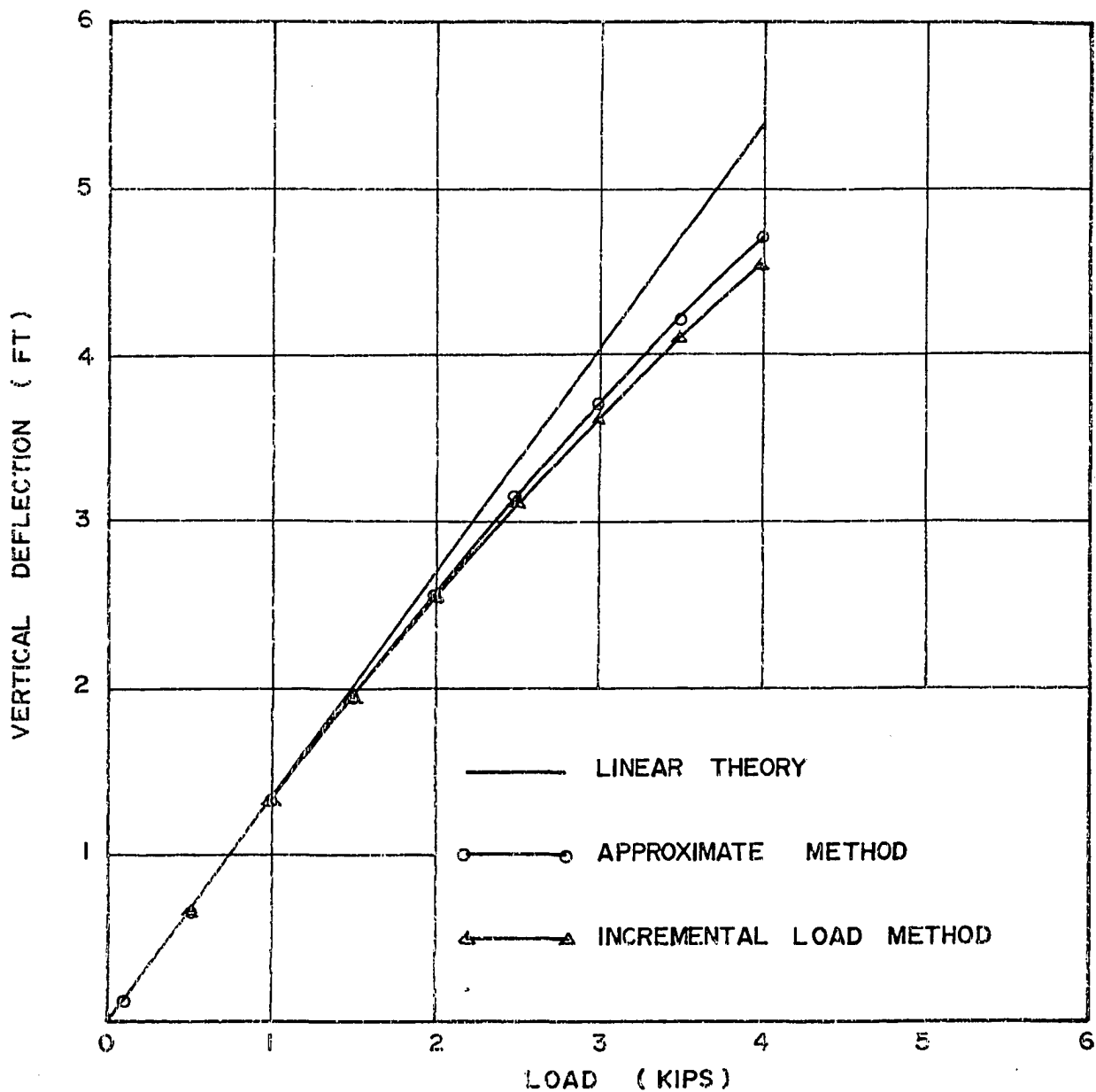


Fig.(5-4)- Deflection at Joint 16 of the 240 ft x 120 ft Cable roof under a Uniform Load.

($H=50$ Kips, $EA=30 \times 10^3$ Kips)

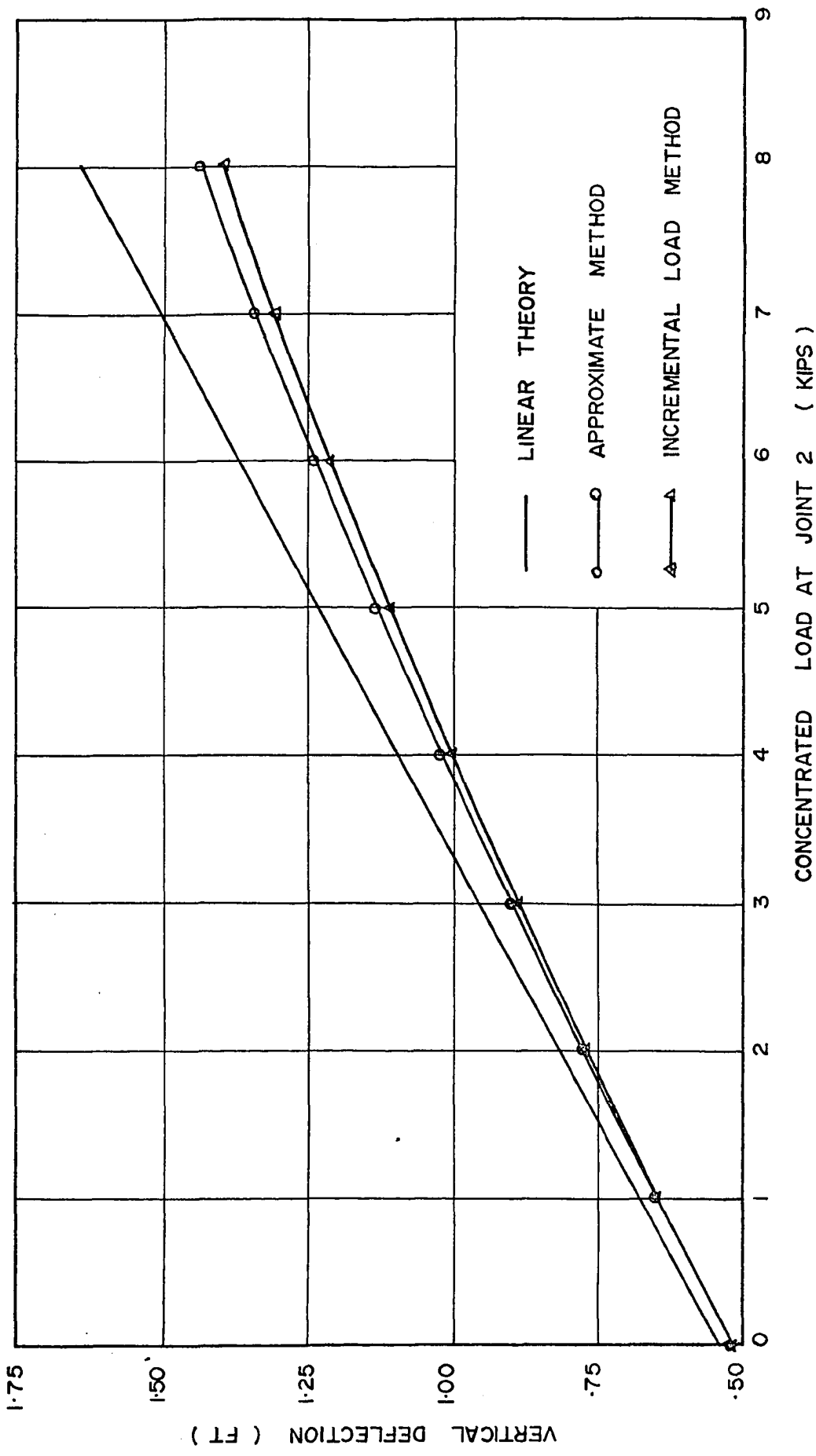


Fig.(5-5) - Deflection at Joint 2 of the 240 ft x 120 ft Cable Roof under a uniform Load of 1 Kip/joint, and a concentrated Load at Joint 2. (H=50 Kips, EA=30x10³)

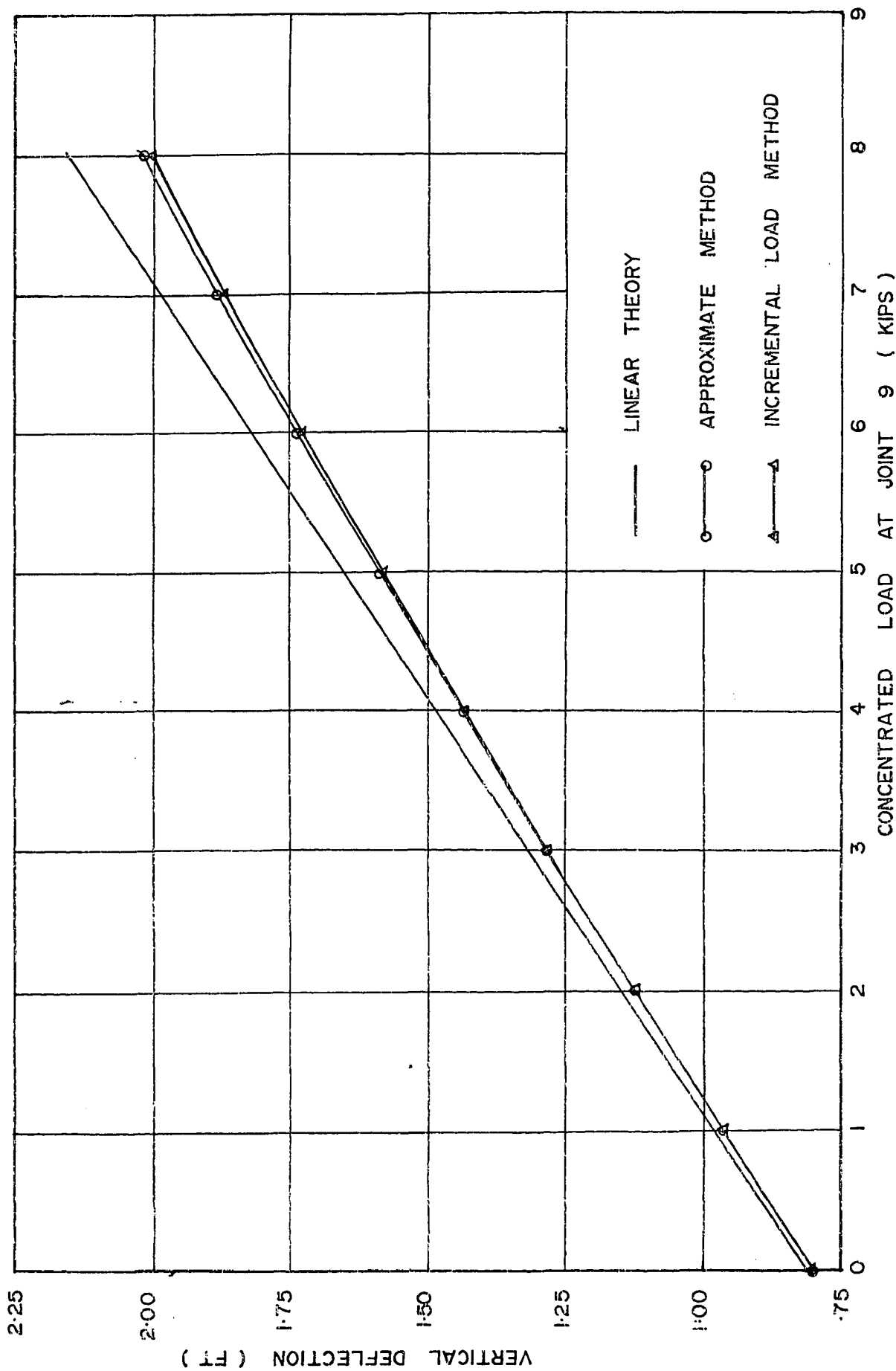


Fig. (5-6) - Deflection at Joint 9 of the 240 ft x 120 ft Cable roof under a Uniform Load of 1 Kip/joint₃ and a Concentrated Load at Joint 9. (H=50 Kips, EA=30x10³ Kips.)

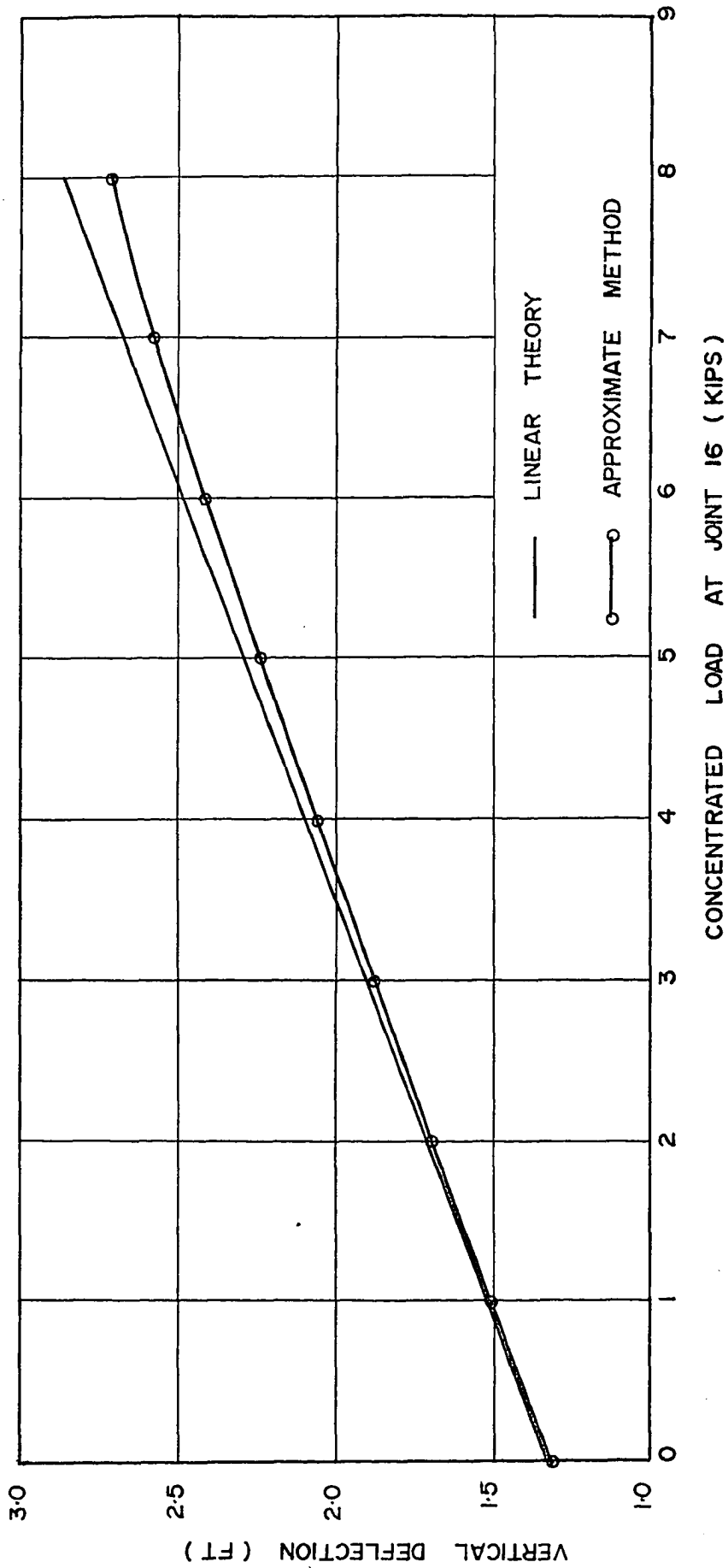


Fig. (5-7) - Deflection at Joint 16 of the 240 ft x 120 ft Cable Roof under a Uniform Load of 1 Kip/joint, and a Concentrated Load at Joint 16. (H=50 Kips, EA=30x10³ Kips.)

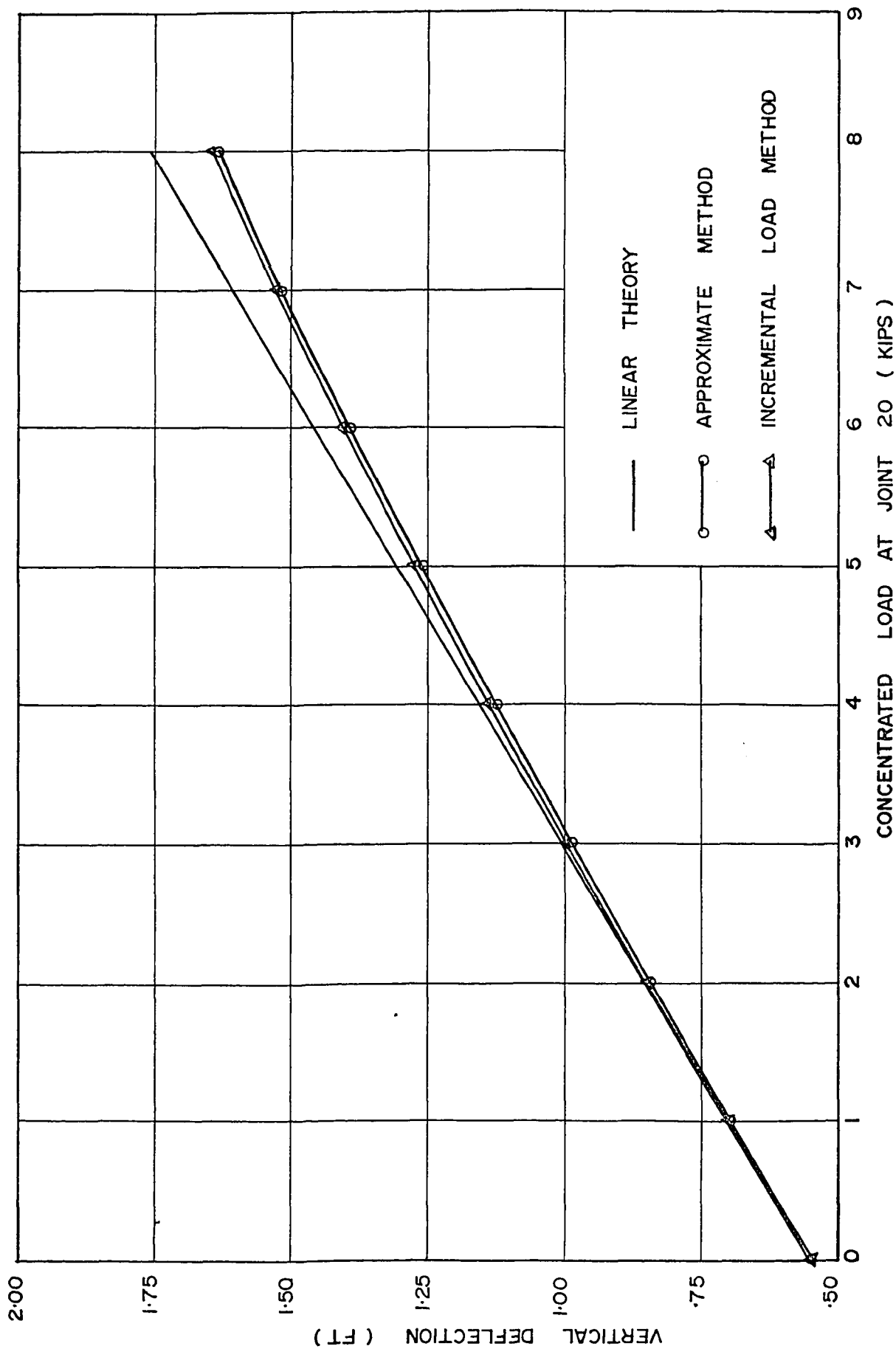


Fig.(5-8)- Deflection at Joint 20 of the 240 ft x 120 ft Cable Roof under a Uniform Load of 1 Kip/joint and a Concentrated Load at Joint 20.

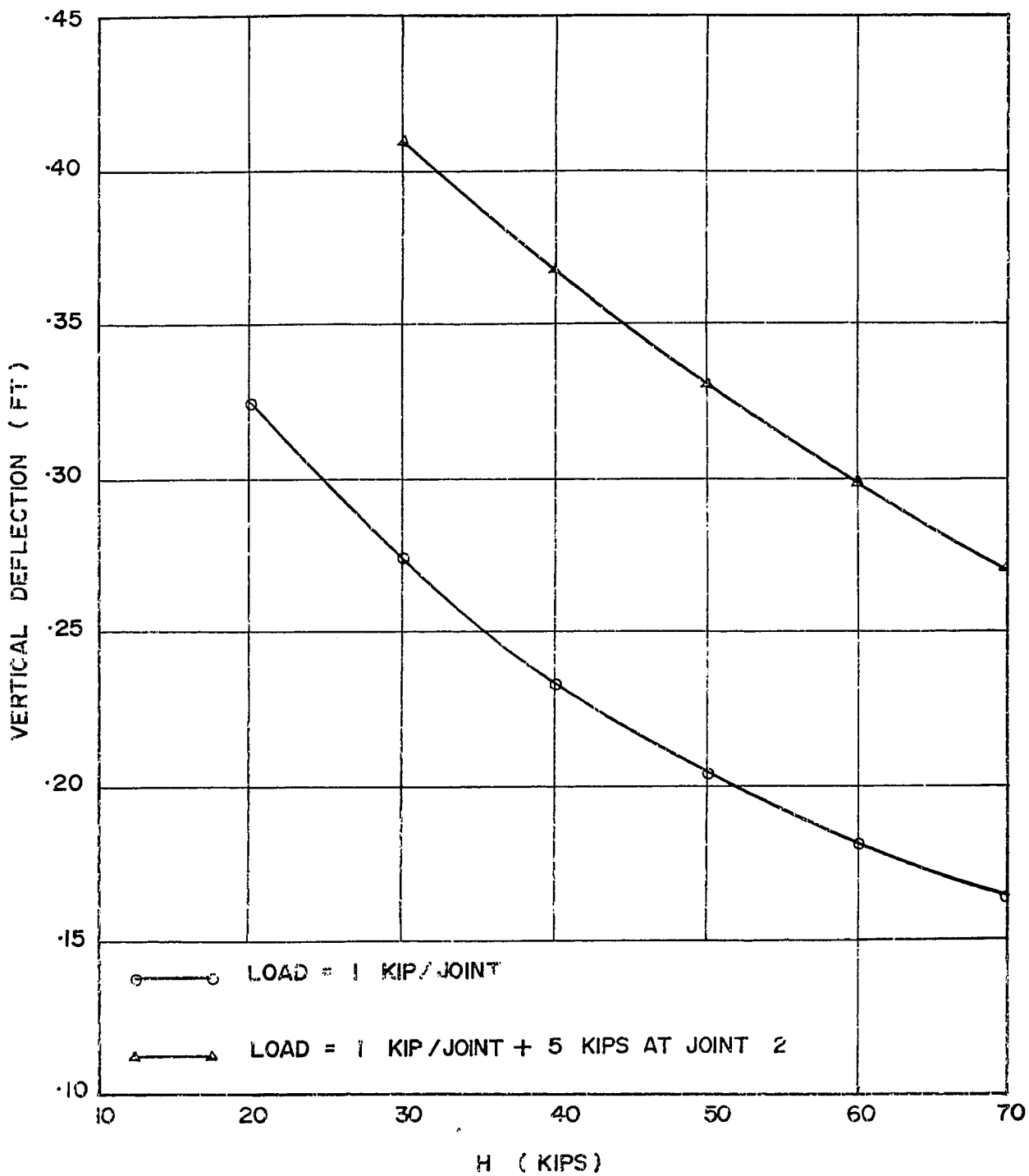


Fig.(5-9)- Variation of the Deflection at Joint 1 of the
240 ft x 120 ft Cable Roof with H. ($EA=30 \times 10^3$ Kips)

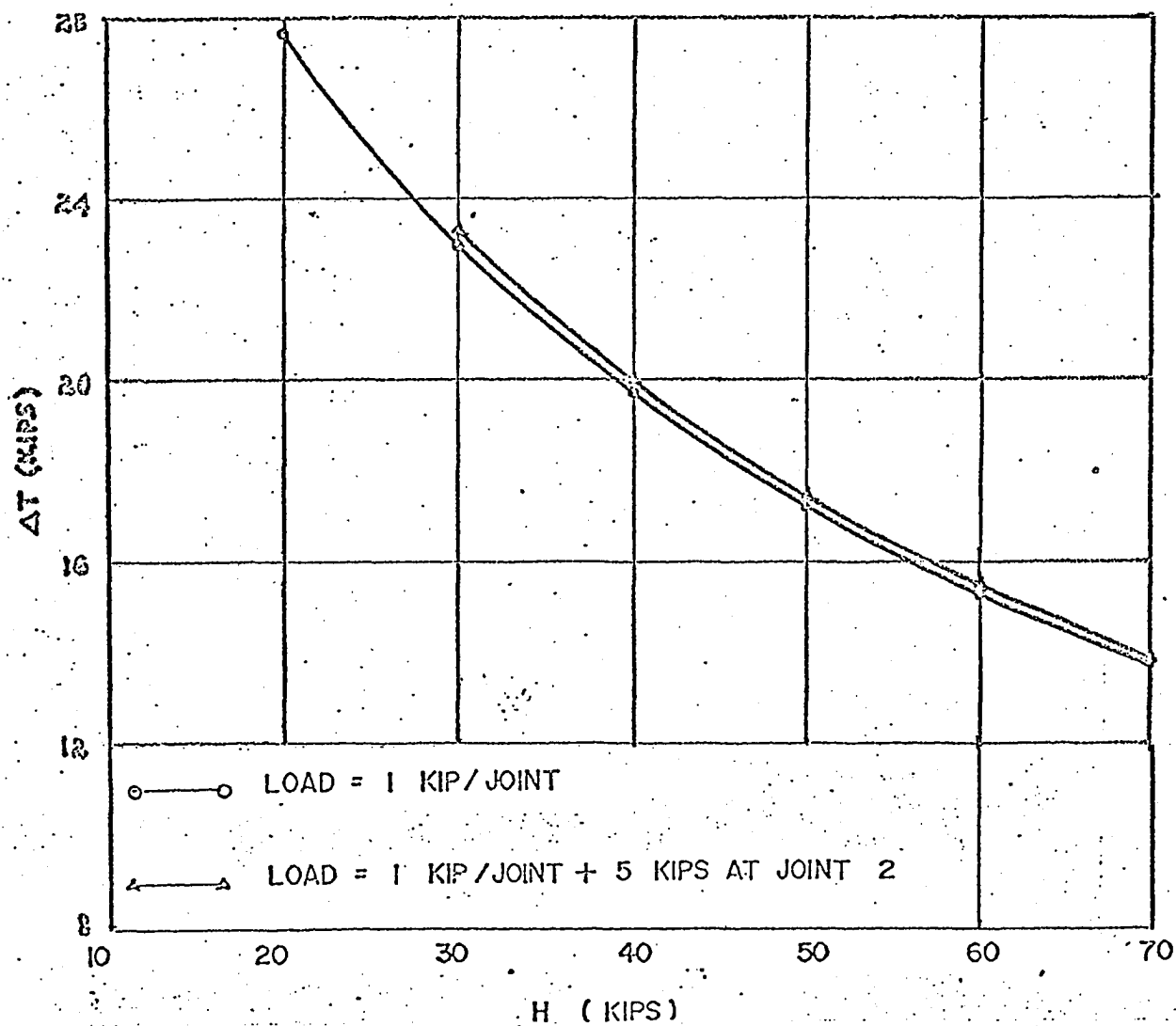


Fig.(5-10a)- Variation of the Tension Increment in the Section of the Cable between Joints 16 and 17 of the 240 ft x 120 ft Cable Roof with H. ($EA=30 \times 10^3$ Kips)

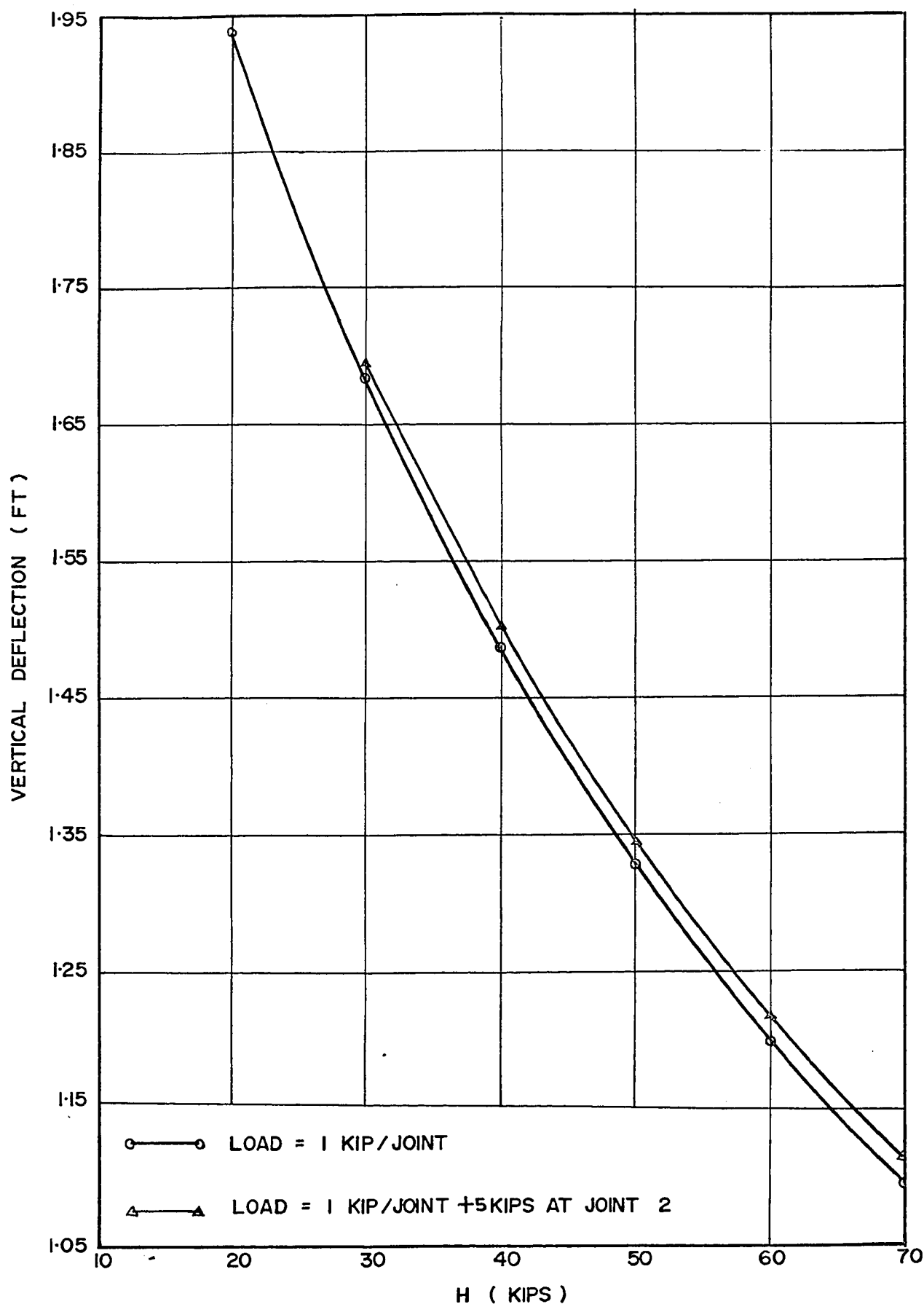


Fig.(5-10)- Variation of the Deflection at Joint 16 of the
240 ft x 120 ft Cable Roof with H. ($EA=30 \times 10^3$ Kips)

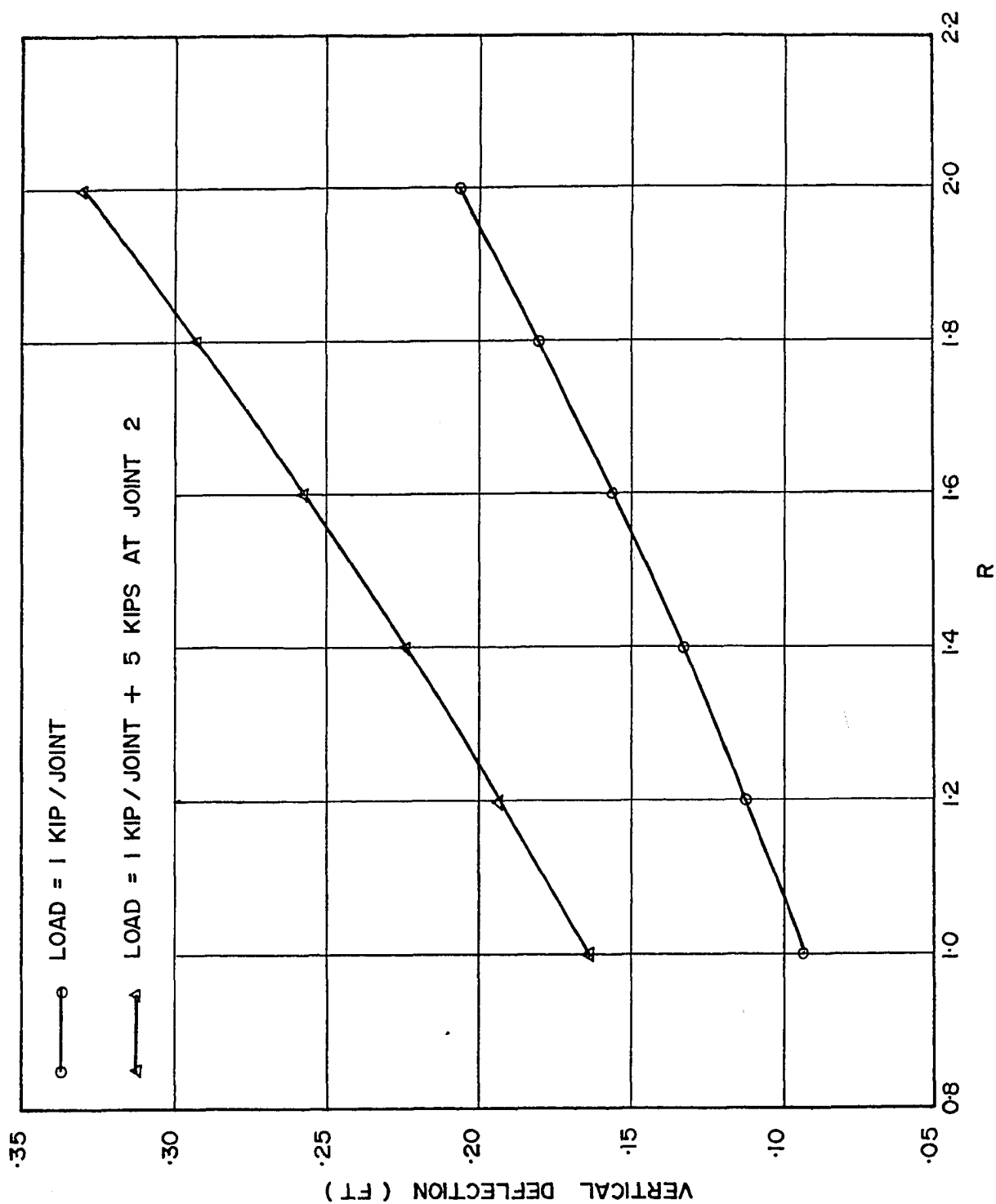


Fig.(5-11)- Variation of the Deflection at Joint 1 of the Cable Roof with R. ($H=50$ Kips, $EA=30 \times 10^3$ Kips)

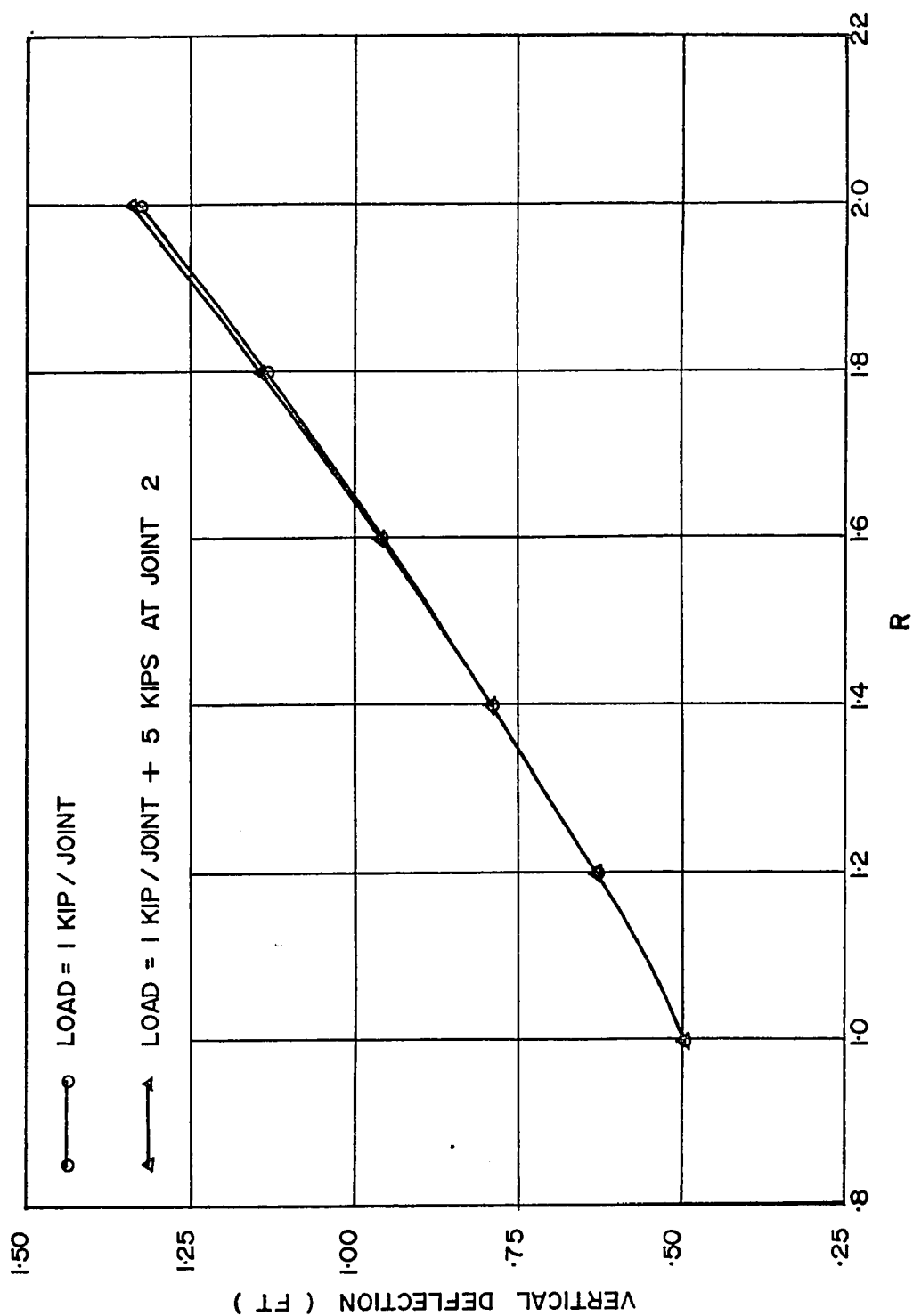


Fig.(5-12)- Variation of the Deflection at Joint 16 of the Cable Roof with R. ($H=50$ Kips, $EA=30 \times 10^3$ Kips)

chapter 6- Experimental Study

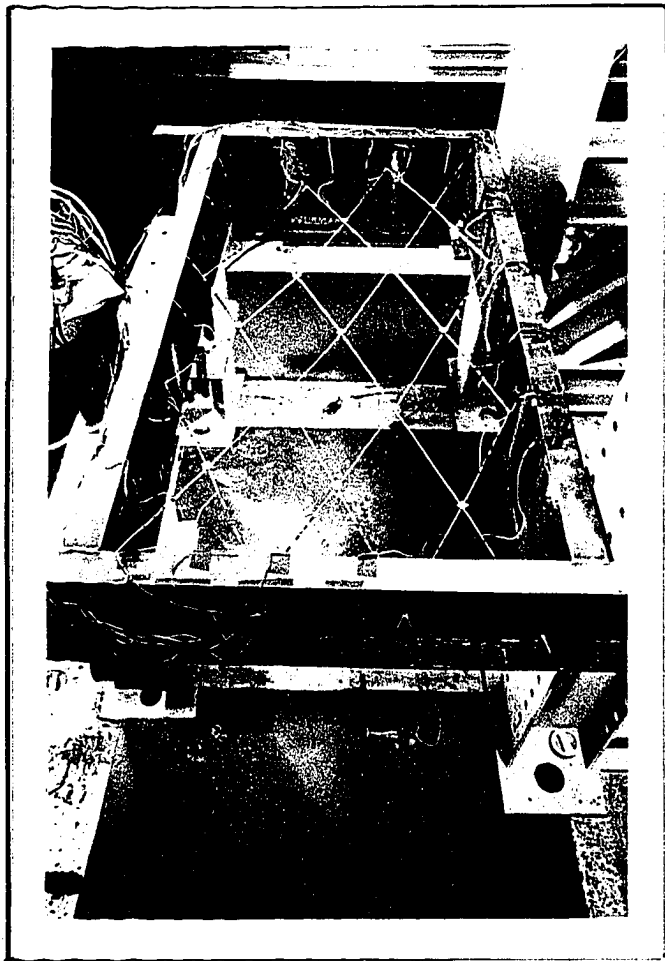
6.1 Description of Model.

In order to verify the theory and calculations, an experiment was performed on a small scale model. The model was 6 ft x 3 ft with a difference in height of 9 ins. between adjacent corners. The net consisted of five 1/8 in. diameter aluminum wires in each direction. The bounding frame was of four 12 in. deep channels welded to form a rectangular box. Holes were drilled on the channels diagonally and along straight lines to form the boundary of the model roof. The wires were provided with screws at the ends for tensioning. The wires were glued together at the joints and hangers were suspended from the joints for loading the net.

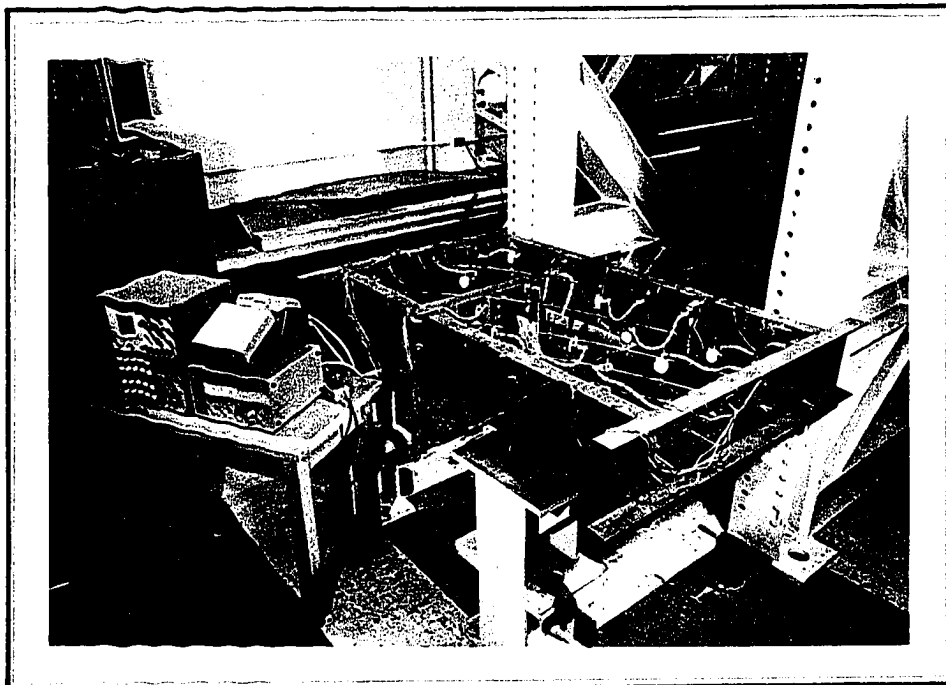
The two sets of wires approximately took the shape of parabolas, with the two sets having opposite curvature. The total number of interior joints were thirteen and heavy channels used for the frame justified the assumption of no frame deformation. The tensions in the wires were measured by attaching strain gauges on the wire at the ends. The deflections were measured by dial indicators.

A plan of the net is shown in fig.(6-1).

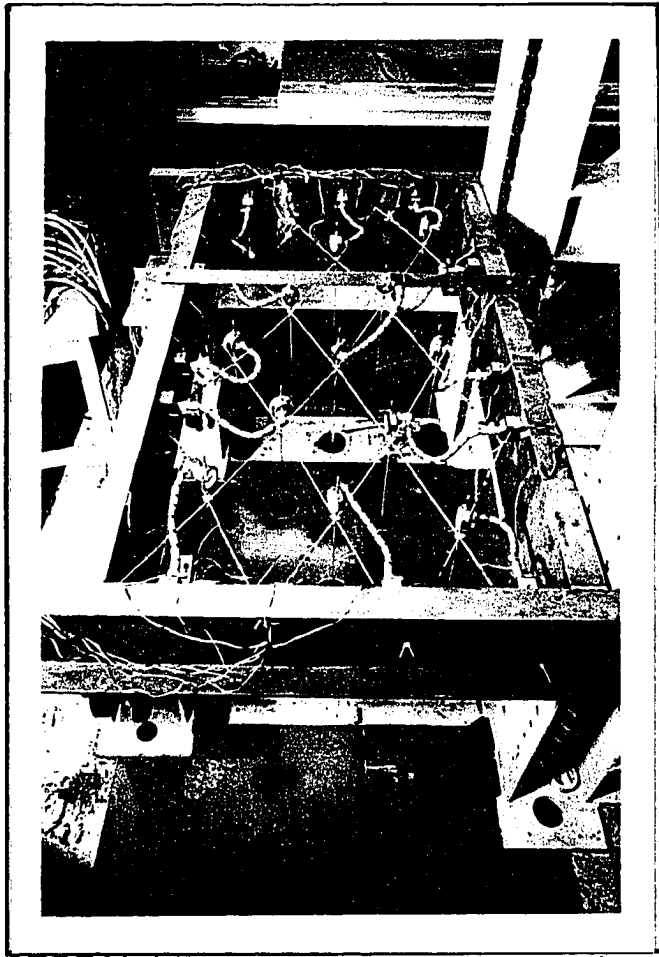
Photographs 1 to 4 illustrate the model.



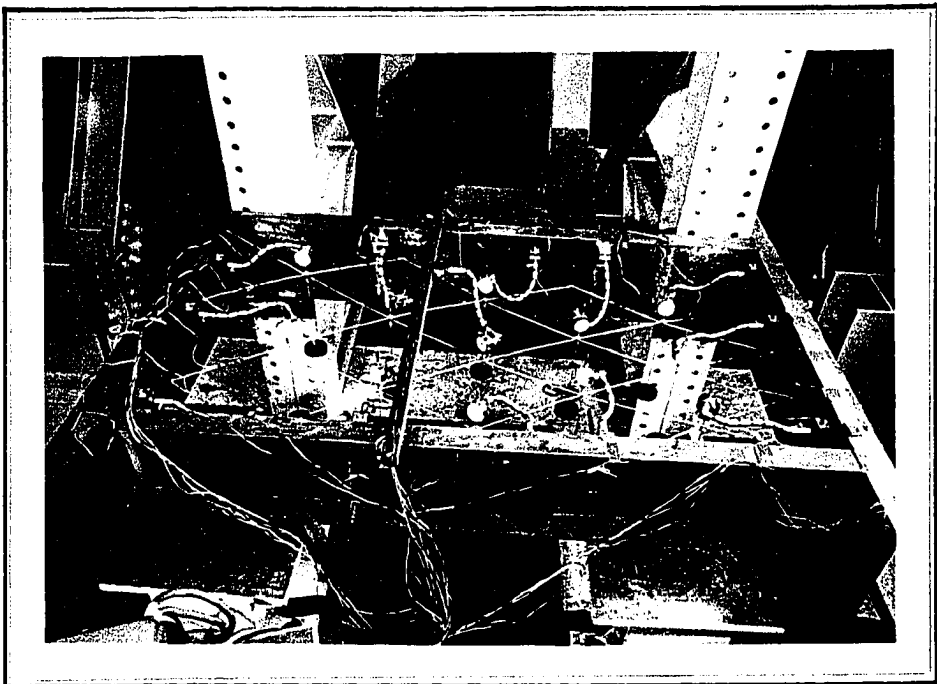
Photograph 1- Top View of the Unloaded Model



Photograph 2. A View of the Loaded Model and the Datran Strain Indicating Equipment.



Photograph 3- Top View of the Loaded Model



Photograph 4- Side View of the Loaded Model.

6.2 Experimental Procedure.

The wires were tensioned and the strains in the wires were checked until the necessary tensions in the wires were reached. The tensions in the wires were so adjusted that their horizontal components were all equal to 50 lbs. The dial indicators were then fixed and adjusted to zero and the joints were loaded. The dial indicator readings were noted. The loads were increased by equal increments of 1 lb at a time to a maximum of 5 lbs. The readings were then repeated while unloading.

Readings were also taken for concentrated loads at various joints increasing from 1 lb to 6 lbs in addition to equal loads of 1 lb at all the joints.

The experimental results and the theoretically calculated results for the model are shown in figs.(6-2) to (6-10).

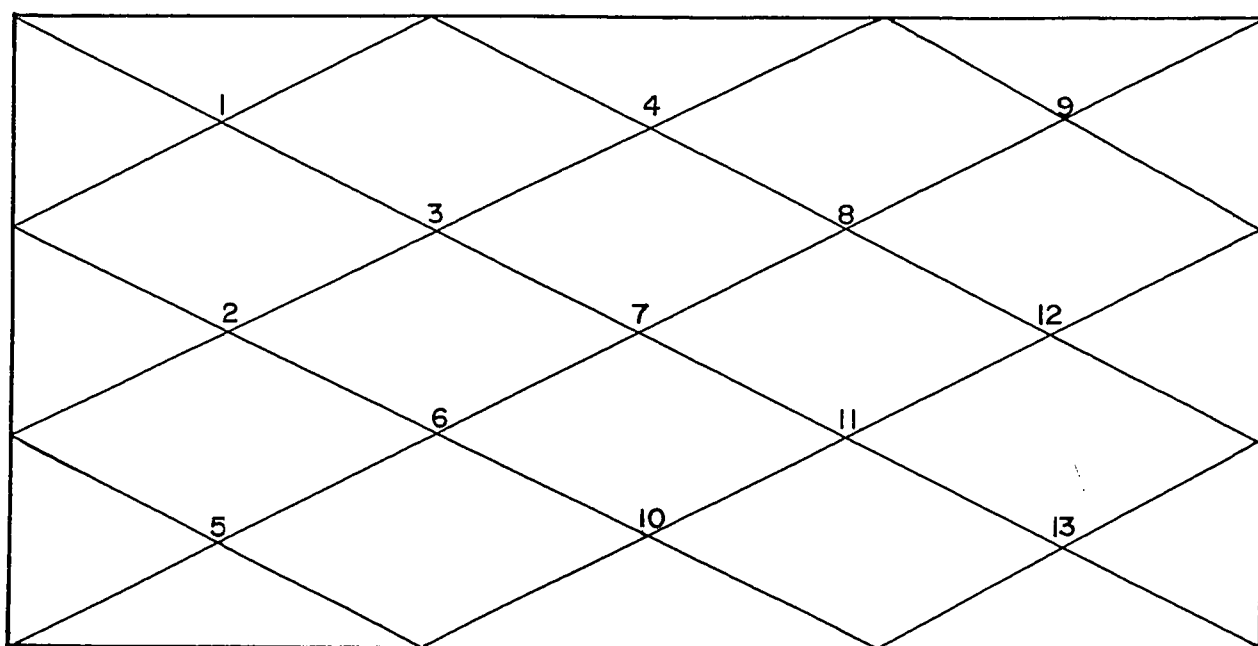


Fig.(6-1)- Plan of Model.

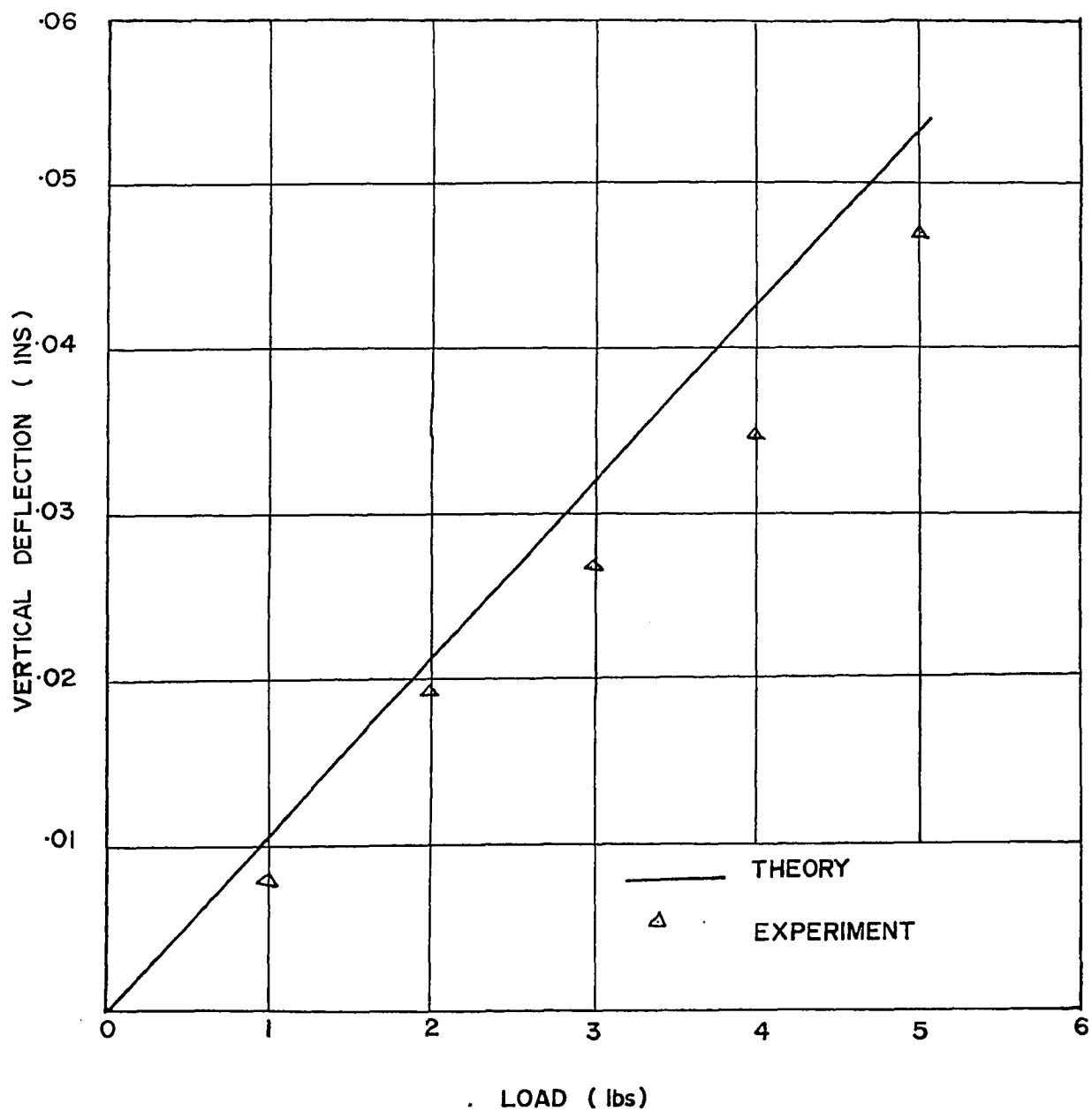


Fig.(6-2)- Deflection at Joint 7 of the Model under a Uniform Load.

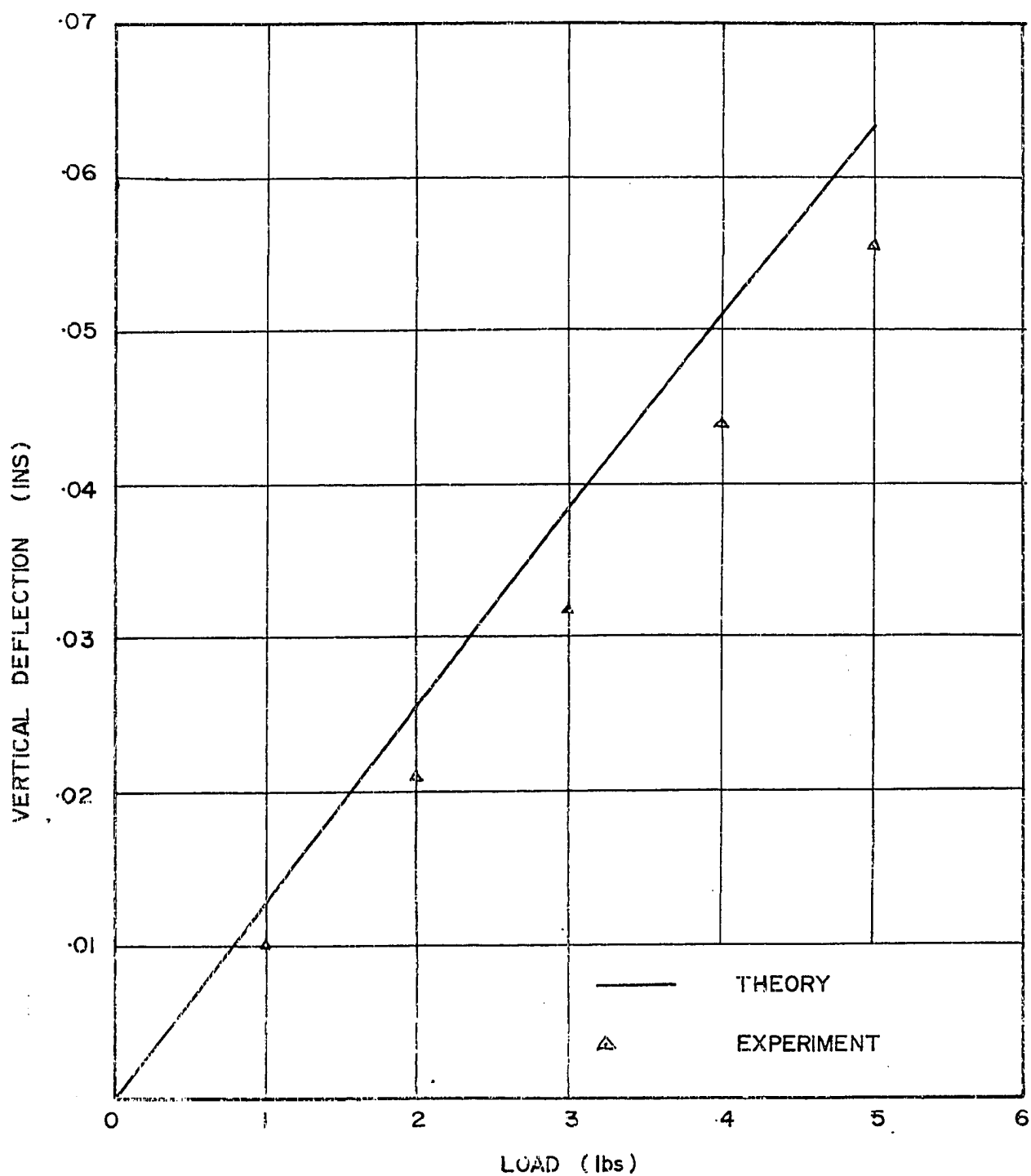


Fig.(6-3)- Deflection at Joint 9 of the Model under a Uniform Load.

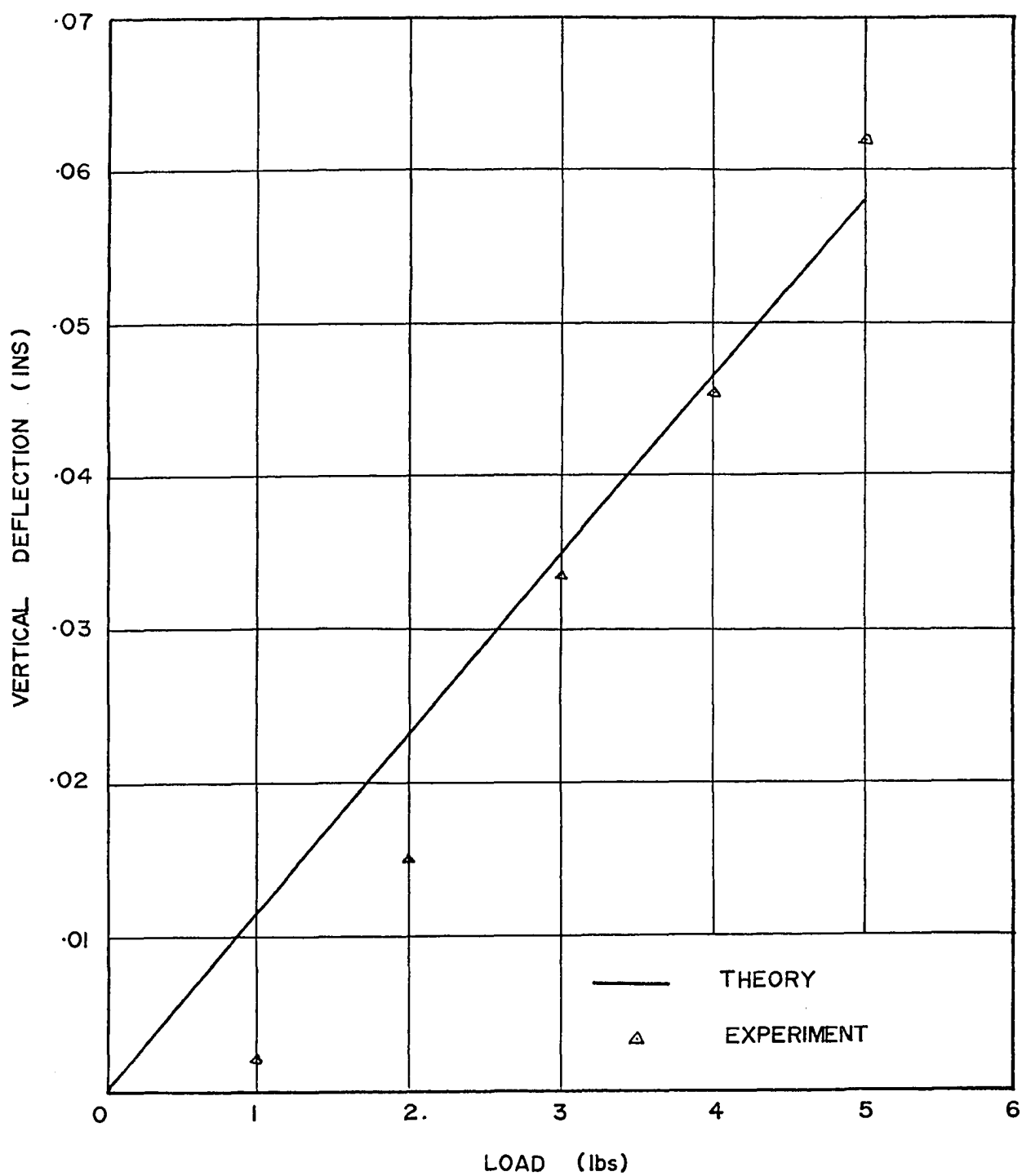


Fig.(6-4)- Deflection at Joint 12 of the Model under a Uniform Load.

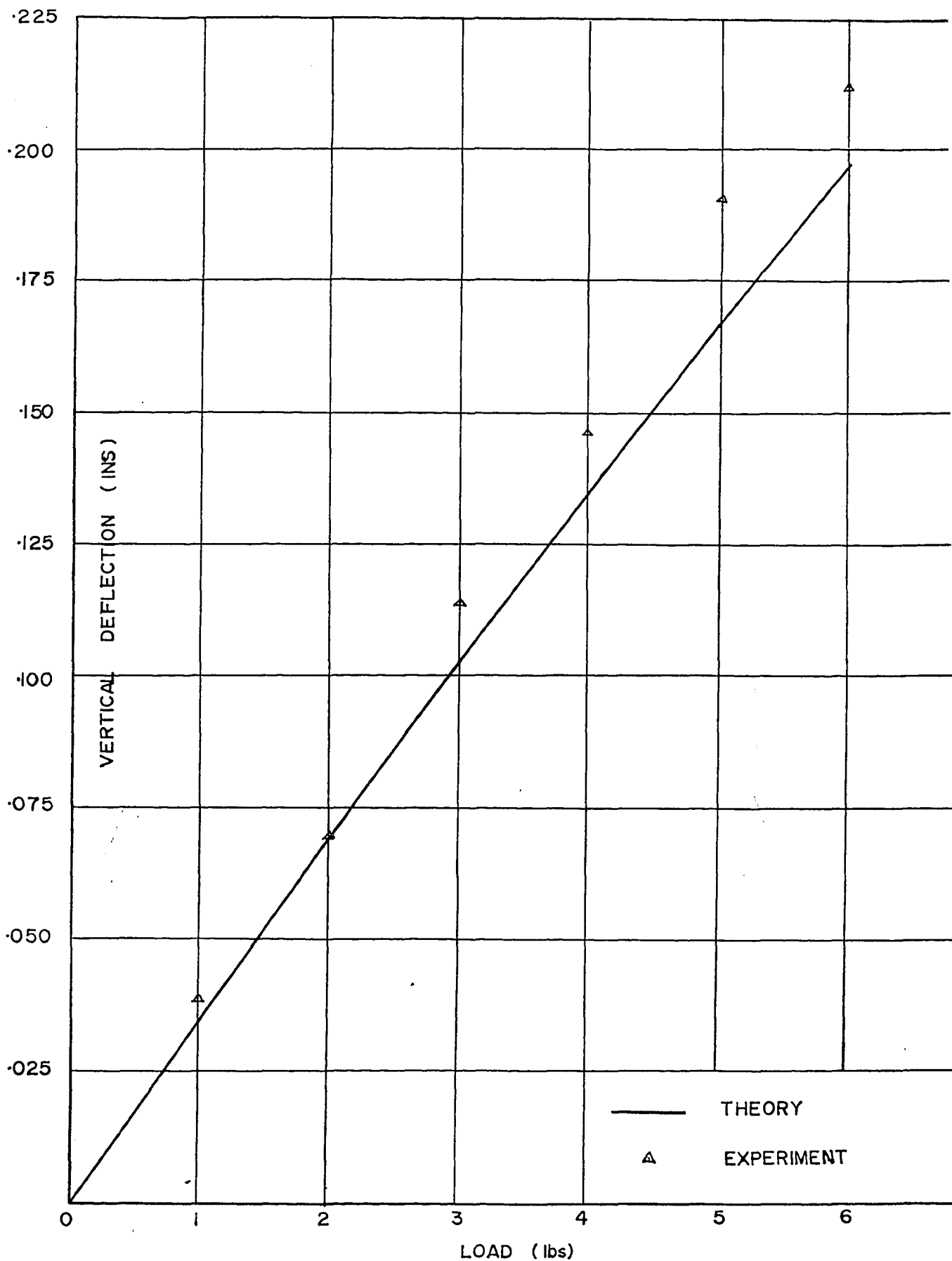


Fig.(6-5)- Deflection at Joint 2 of the Model under a Concentrated Load at Joint 2.

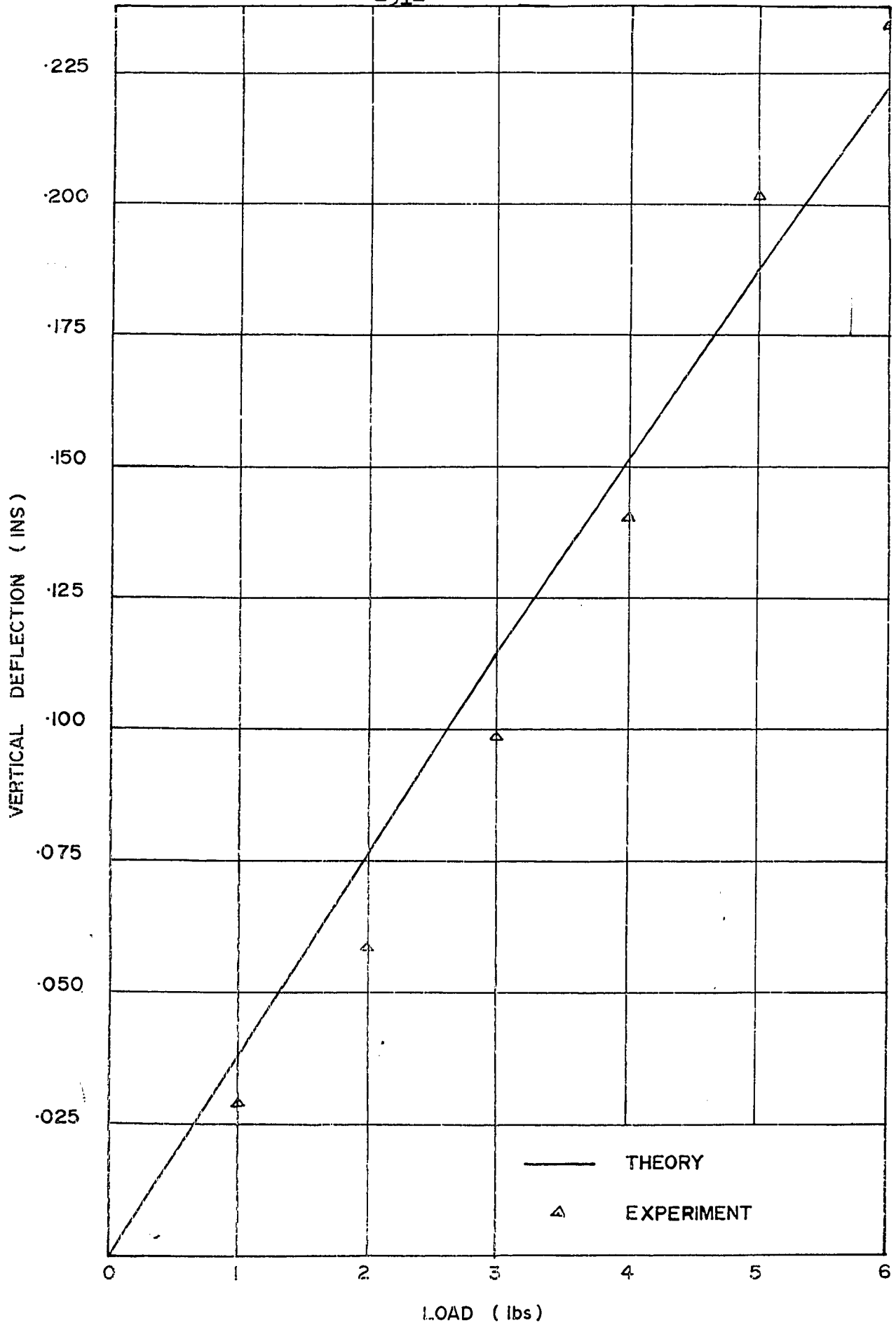


Fig.(6-6)- Deflection at Joint 7 of the Model under a Concentrated Load at Joint 7.

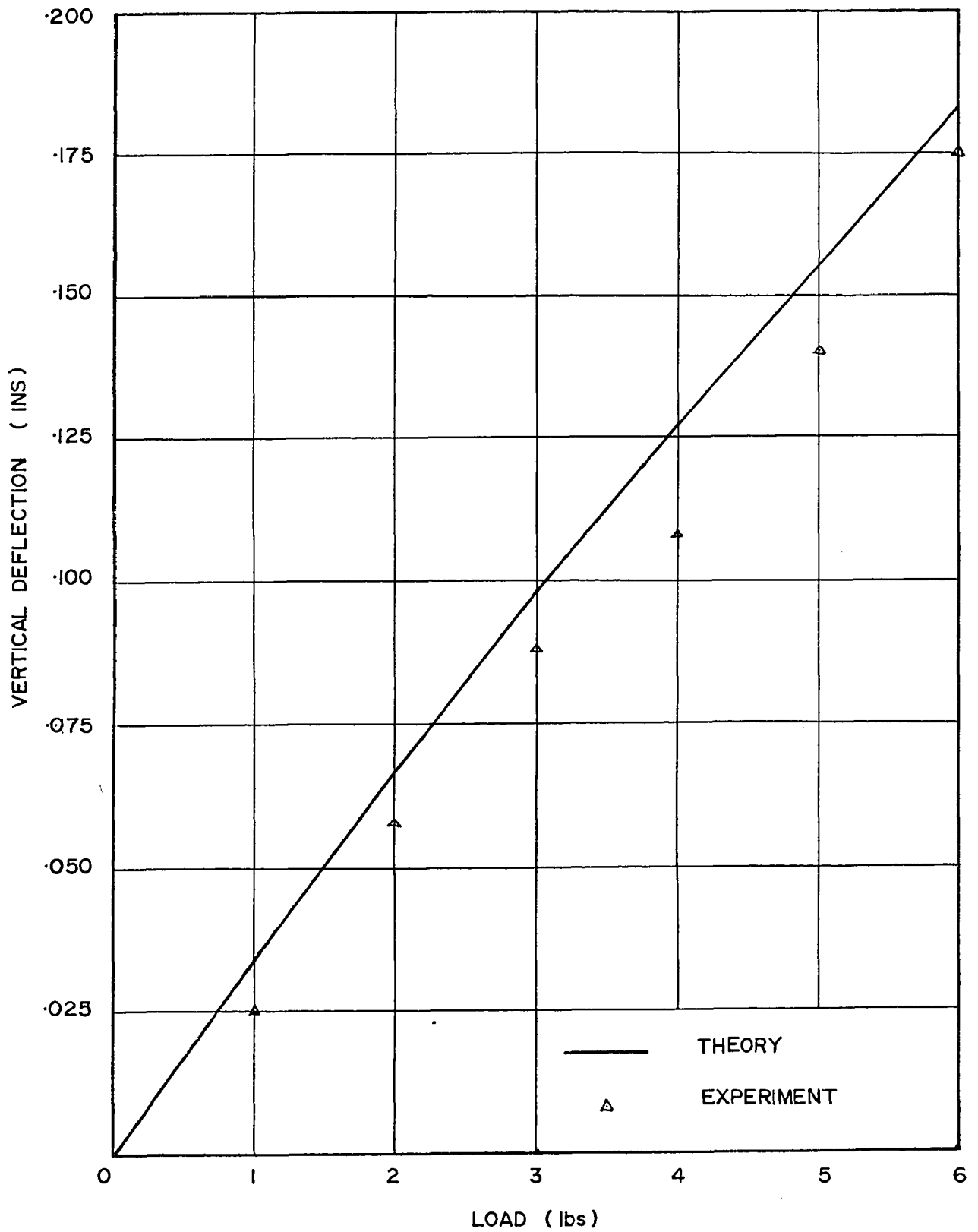


Fig.(6-7)- Deflection at Joint 8 of the Model under a Concentrated Load at Joint 8.

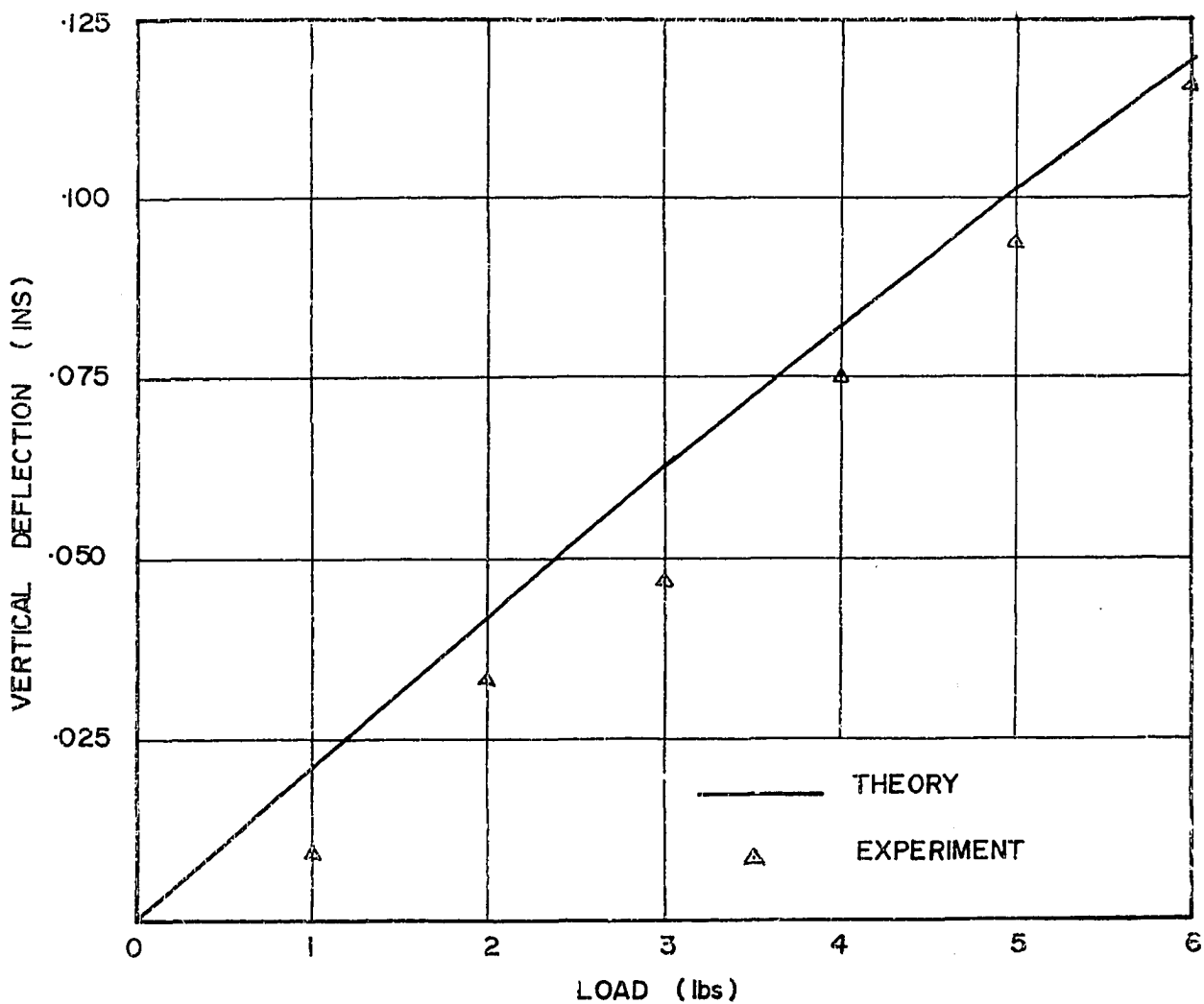


Fig.(6-8)- Deflection at Joint 9 of the Model under a Concentrated Load at Joint 9.

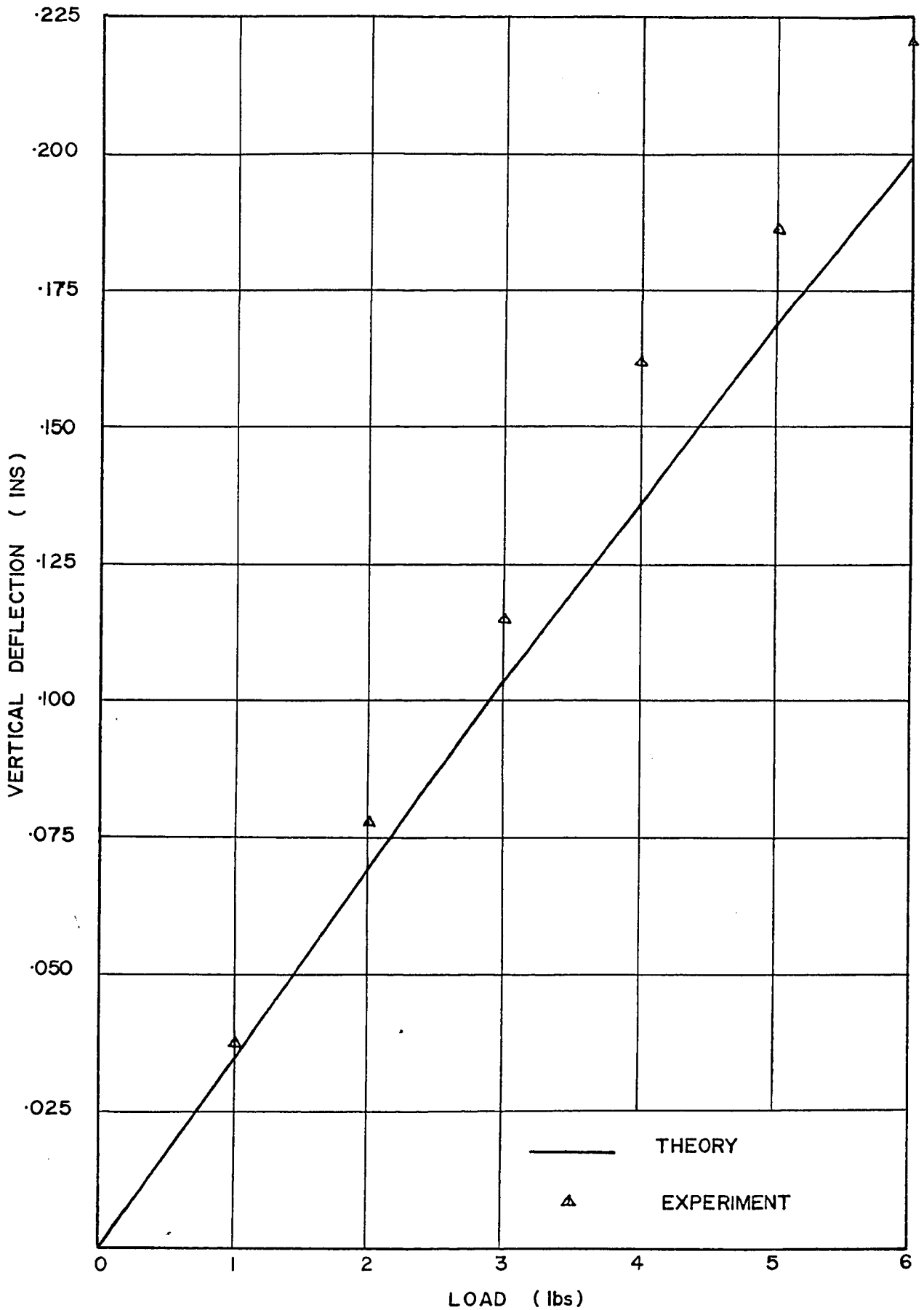


Fig.(6-9)- Deflection at Joint 10 of the Model under a Concentrated Load at Joint 10.

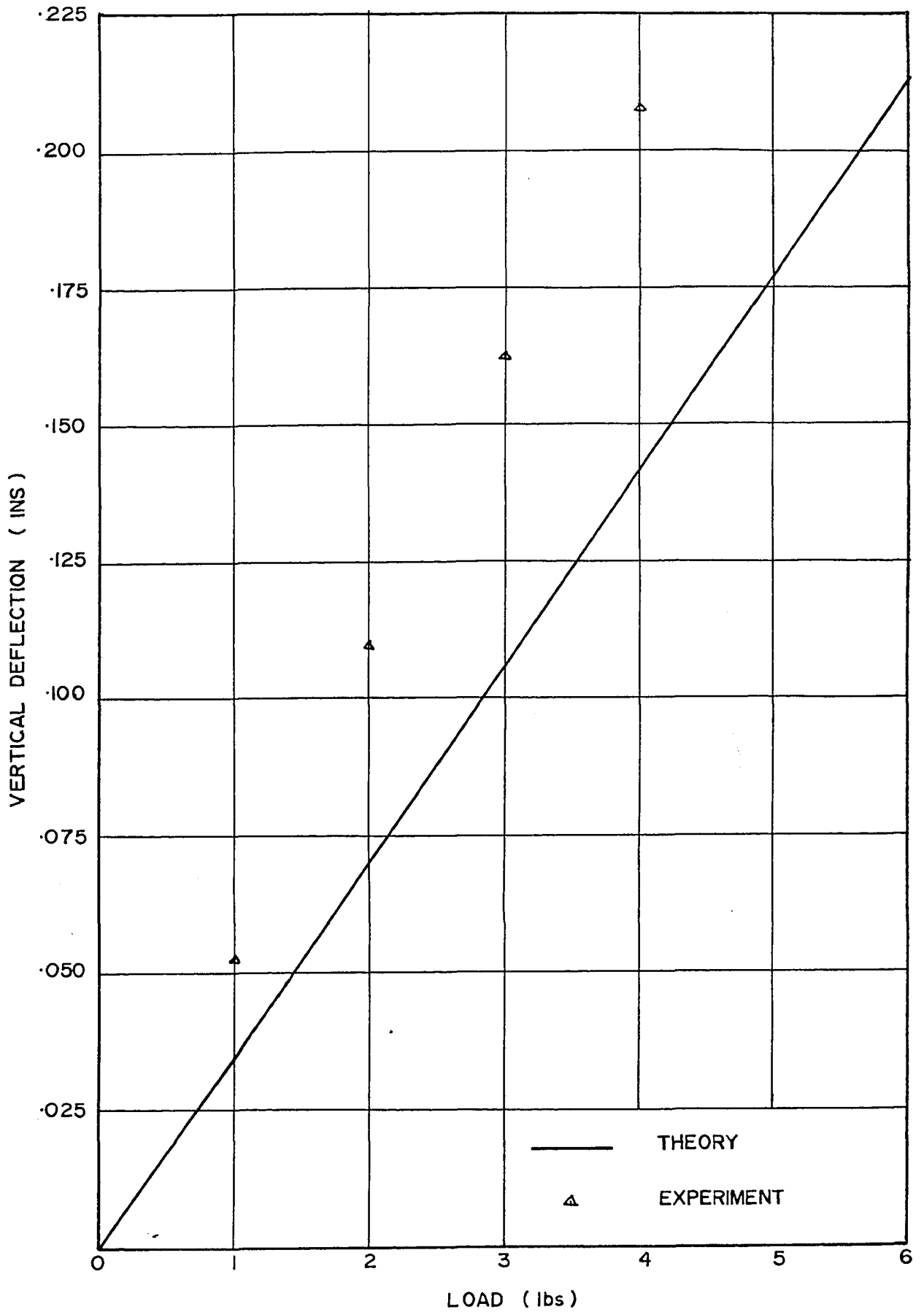


Fig.(6-10)- Deflection at Joint 11 of the Model under a Concentrated Load at Joint 11.

Chapter 7- Discussion of Results.

1. The vertical displacements were calculated using the approximate method neglecting horizontal displacements with the deformation of the frame neglected in one case and with the deformation of the frame taken into account in another. The difference between the calculated values in the two cases will, of course, depend on the stiffness of the frame. In the case considered here, with $E = 30 \times 10^3$ Kips/in² and $I = 3200$ in⁴ there is a maximum difference of 9% between the two displacements but for most of the joints, the difference is about 4%. Whether or not it is necessary to consider the deformation of the frame depends on the stiffness of the frame actually used.
2. The vertical displacements when calculated using the general theory taking horizontal displacements into account, differ from the values calculated by the approximate theory by a maximum of 6%. In addition to this difference, the horizontal displacements which were neglected in the latter theory are significant, approaching 5 to 7% of the vertical displacements when the former theory is used. These two differences combine together to give a larger error in the calculated tension increments. Such increments in the two cases differ by up to 12% in the longer cables where the change in tension is large. It is therefore necessary that the general theory be used in the analysis of this type of roof in order to

obtain accurate results, even though this involves three times the number of equations.

3. It is also evident from the graphs [figs. (5-3) to (5-8)] that the load deflection behaviour is nonlinear for loads larger than 1 Kip/joint for the roof considered here. Increasing load has a 'strengthening' effect on the net, i.e. the corrected value is lower than the value obtained by the linear theory. For smaller loads, it would be sufficient to use the linear theory but for larger loads, this would result in a conservative value for displacements and the tension increments.

4. It is seen from the calculations that the value obtained by the approximate method of correction for nonlinearity almost coincides with the value obtained by the more accurate incremental load method. The difference between the two values is greatest when the loading is unsymmetrical [fig. (5-5)] but is negligibly small in the case of symmetrical loading [fig. (5-6)]. It is sometimes timesaving to use the former, since in most cases one is interested in the displacements under a particular loading in which case solution by the former will require a few iterations whereas the latter might require several increments to reach the particular value of loading. The values obtained by the two methods deviate more as the load increases but the amount of computing time taken with the incremental load method over and above the approximate method, also increases with the load and offsets the advantage of the slightly more accurate results. For example, for equal

loads of 4 Kips/joint, the first method requires 15 iterations to converge within 1×10^{-6} , while the incremental load method requires 40 increments of 0.1 Kips each and the difference between the two values is only about 3% for a saving of 60% of the computing time.

5. From a comparison of the deflection of joint 2 due to a concentrated load at joint 2 and the deflection of joint 20 due to a concentrated load at joint 20, it is seen that the nonlinearity is more marked when the loading is unsymmetrical.

The former is unsymmetrical while the latter is symmetrical since it assumes a concentrated load in the opposite corner.

6. The deflections and tension increments decrease with the increase of H, the horizontal component of tension, as expected. The deflections could be reduced by increasing the pretension in the cables but this increased tension will have to be accounted for at the edge beams and the anchorages. A compromise, therefore, has to be struck and other factors such as susceptibility to flutter also must be considered.

7. The deflection decreases as the degree of nonorthogonality of the net decreases and is a minimum when the net is orthogonal. The horizontal displacements are also much smaller in the orthogonal net than in a nonorthogonal net.

8. The experimental values agree with the theoretically calculated values within reasonable limits. The difference between the theoretical and the experimental values differ by very small to large percentages but the average difference can be said to be about 10-15%. The theoretical values are on

the conservative side for most cases of loading and for most of the joints. This is seen from figs.(6-2), (6-3) and (6-4) for symmetrical loading and from figures (6-6), (6-7) and (6-8) for concentrated loads at joints 7,8 and 9 respectively. The theoretical values are lower than the experimental values only in the case of concentrated loads at joints 2,10 and 11 [figs.(6-5), (6-9) and (6-10)]. Since these latter joints are less critical than the former joints from the design point of view and since the theoretical values are on the conservative side for most cases of loading, it may be said that in general the theoretical values are on the conservative side.

9. The sources of error in the experiment may be one or more of the following:-

- (a) Inaccuracy in measuring the initial tension in the wires and the value of EA used.
- (b) Irregularity in the geometry of the model.
- (c) Stiffness of the joints and the bending stiffness of the wires which were neglected in the theory.
- (d) Any deformation of the frame.
- (e) Inaccuracy in measuring the deflections.
- (f) Inaccuracy of the theory.

Source (a) is likely because there would have been an error in the measurement of the strain with the strain gauges. A non-axial strain gauge alignment can introduce significant error. The value of E used was the value supplied by the manufacturer for 6061 T6-H19 aluminum which was used.

Source (b) is also likely due to irregularities in fabricating the model and due to the finite thickness of the wire and the joints.

The stiffness of the glued joints and the bending stiffness of the wires would also introduce some error. The measured deflection would have been somewhat inaccurate due to friction in the dial indicators but this was eliminated to some extent by using the average value of the readings taken while loading and unloading. The deformation of the frame could not have introduced any significant error, considering its excessive rigidity. The theory too cannot be called inexact since it is derived from first principles considering the equilibrium of the system. Correction for nonlinearity was applied by incremental load method and noting the very small nonlinearity of the system, the error involved would be negligible.

10. Since the nonlinearity of the model was smaller than the accuracy with which the experimental results were obtained, the nonlinear behaviour of the model could not be verified.

Chapter 8- Conclusions.

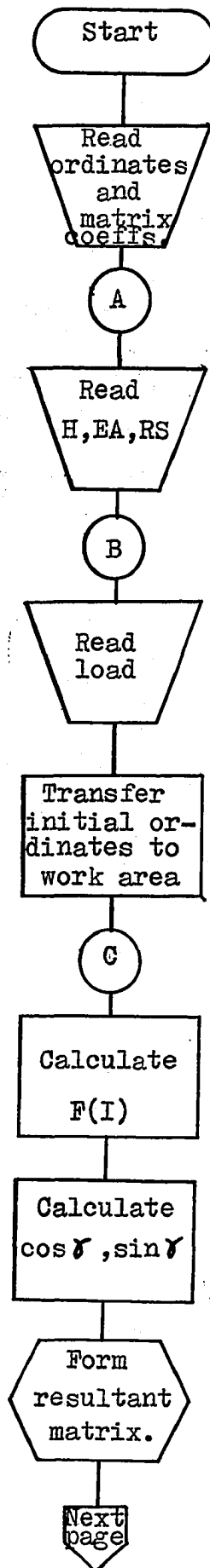
For the study presented herein, the following conclusions can be drawn:-

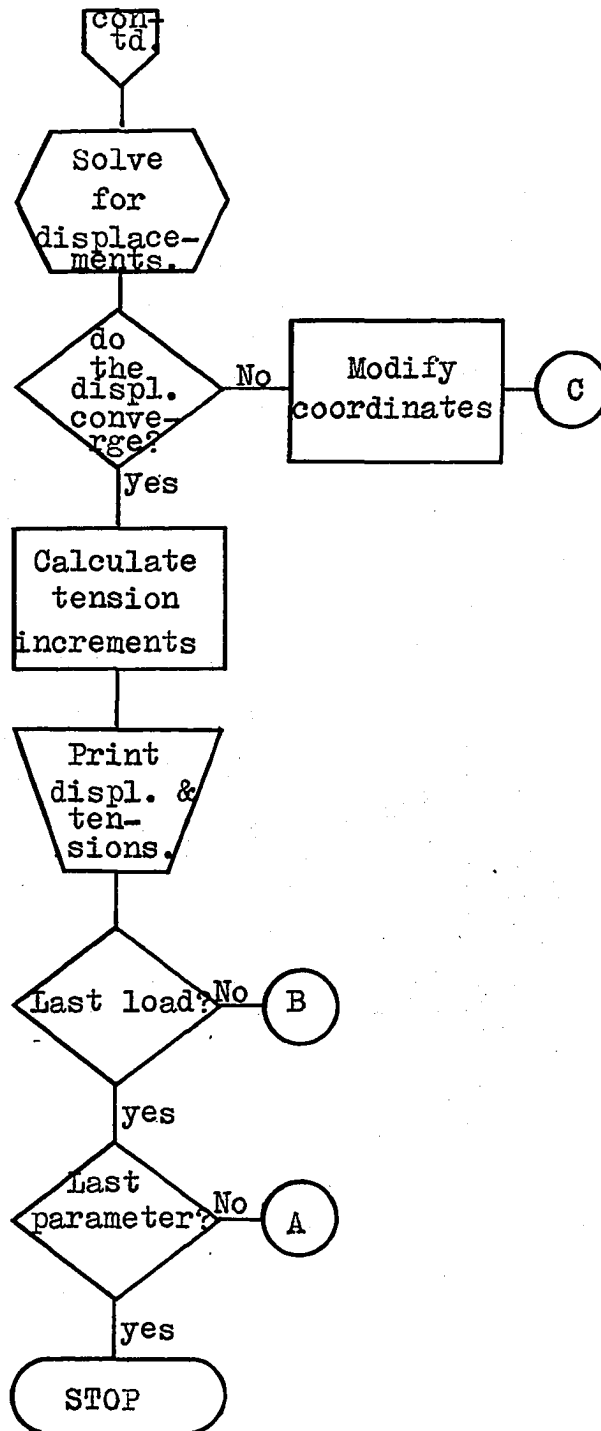
1. For nonorthogonal nets the horizontal displacements cannot be neglected in comparison to the vertical displacements. Therefore the general theory considering displacements in all directions has to be used. In the case of orthogonal nets, however, the horizontal displacements are small and may be neglected.
2. In calculating the vertical displacements of the joints, the effect of deformation of the bounding frame may have to be taken into account depending on the flexural rigidity of the edge beam used. This may become necessary in the case of very long spans where the edge beam is used without intermediate supports.
3. The load-deflection behaviour is nonlinear for large loads. In applying correction for nonlinearity, the value obtained by using the approximate method is not very much different from that obtained by the incremental load method. The former may be used in favour of the latter on account of the appreciable saving in computing time for any one particular set of loading. Furthermore, the nonlinearity is more marked in the case of unsymmetrical loading.
4. The deflections and tension increments decrease with the

increase in pretension. They also decrease with the nonorthogonality of the cables.

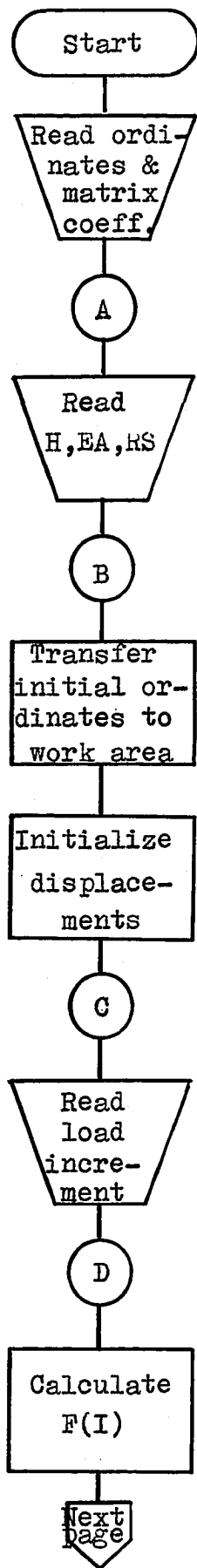
5. The experimental values are in fair agreement with the theoretical values. The theoretical values are in general on the conservative side. Nonlinear behaviour could not be verified experimentally due to the very small nonlinearity of the model used. For future work, it is recommended that a more flexible model be used so that the nonlinear behaviour of the system could be more readily verified.

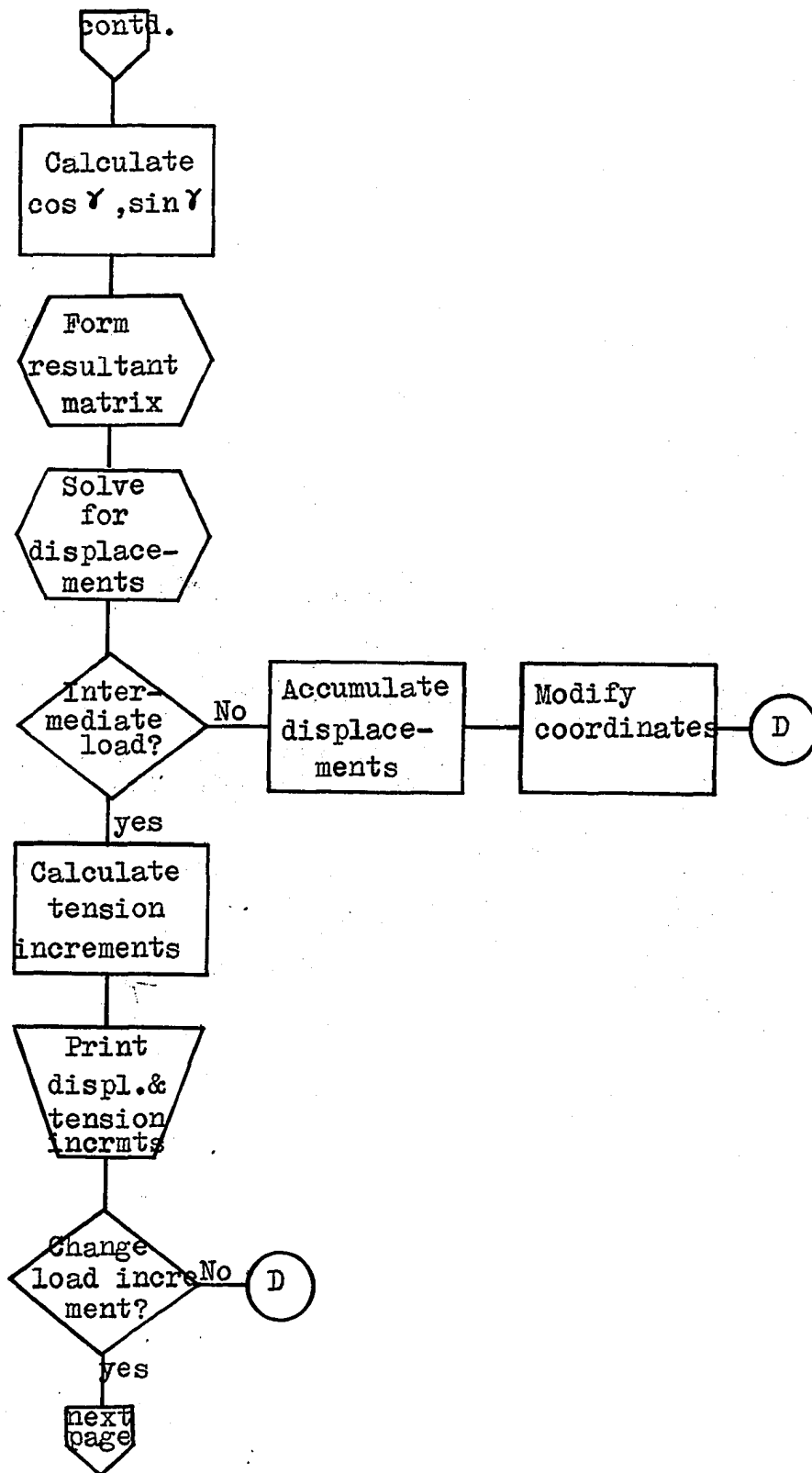
Appendix A- Flow Charts for Computer Programs.

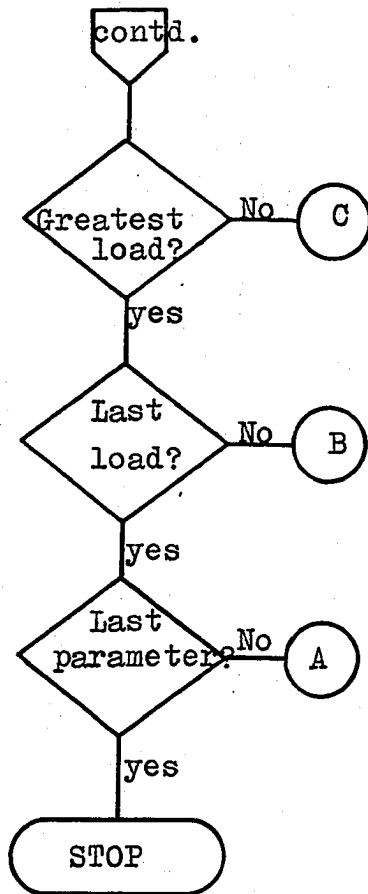




Flow Chart 1- Calculation of Displacements-Correction for Nonlinearity by Approximate Method.







Flow Chart 2- Calculation of Displacements- Incremental Load Method.

APPENDIX B. LISTING OF A SAMPLE PROGRAM.

```
//CONLOAD JOB 1 00005,KUMARAN,MISLEVEL=1
//EXECCLG EXEC FORTCLG,PARM.FORTCLG
//FORT.SYSIN DD *
C T.KUMARAN DEPT. OF CIVIL ENGINEERING
C NON-ORTHOGONAL CABLE ROOF
C GENERAL ANALYSIS, INCREMENTAL LOAD METHOD
C CONCENTRATED LOAD
C
C 1. READ INPUT DATA
C
  DIMENSION AX1(36,36),AX2(36,36),AX3(36,36),AX4(36,36),AX5(36,36)
  DIMENSION AM1(108,108),AM2(108,108),AMX(108,108)
  DIMENSION B(108),B1(108),Z(36),Z1(36),F(6),SUM(6),R(6),DIS(108)
  DIMENSION COSG(36,4),SING(36,4),DELT(36,4)
  READ 110,(Z1(I),I=1,36)
110 FORMAT (3F12.9)
  READ 120,((AX1(I,J),J=1,36),I=1,36)
  READ 120,((AX2(I,J),J=1,36),I=1,36)
  READ 120,((AX3(I,J),J=1,36),I=1,36)
  READ 120,((AX4(I,J),J=1,36),I=1,36)
120 FORMAT (18F3.0)
  READ 130,(R(I),I=1,6)
130 FORMAT (6F10.8)
140 FORMAT (F5.1,F11.4,F3.1)
  PRINT 150
150 FORMAT (11HINPUT DATA)
155 FORMAT (4HCH= ,F8.1,5X,4HEA= ,F8.1,5X,12HSIN(THETA)= ,F10.8)
160 FORMAT (8HLOAD NO,14/(1H0,18F6.1))
170 FORMAT (10HCOORDINATES/(1H0,9F12.8))
180 FORMAT (10HMAX MATRIX/(1H0,18F6.1))
185 FORMAT (5HCR ,6F10.8)
  PRINT 190
  PRINT 170,(Z1(I),I=1,36)
  PRINT 185,(R(I),I=1,6)
190 FORMAT (8HRESULTS)
C
C 2. CALCULATE F(I)
C
205 READ 140,H,EA,RS
  KLD=0
200 LD=0
  KH=0
  DO 195 I=1,36
195 Z(I)=Z1(I)
  DO 230 I=1,108
230 DIS(I)=0.0
305 READ 120,(B1(I),I=1,108)
  A=10.0*SQRT(1.0+RS**2)
  SINT=(RS**2-1.0)/(RS**2+1.0)
  COST=SQRT(1.0-SINT**2)
  PRINT 155,H,EA,SINT
  DO 220 I=1,6
  SUM(I)=0.0
  DO 210 J=1,I
210 SUM(I)=SUM(I)+R(J)
  SUM(I)=SUM(I)**2
  SQI=I**2
220 F(I)= A*(1.0+8.0/3.0*SUM(I)/((2.0*I*A)**2))
  PRINT 290,A,(F(I),I=1,6)
290 FORMAT (F16.3/(6F16.3))
240 LD=LD+10
```

C
C
C

3. CALCULATE COS(GAMMA), SIN(GAMMA)

```

      KNE=0
300 KT=6
      IA=1
      JA=1
      IS=37
310 I=IA
      J=JA
320 K=I+J
      COSG(K,1)=(Z(I)-Z(K))/F(KT)
      COSG(I,2)=(Z(K)-Z(I))/F(KT)
      COSG(K+1,3)=(Z(K)-Z(K+1))/F(J+1)
      COSG(K,4)=(Z(K+1)-Z(K))/F(J+1)
      IF (JA-1) 323,324,325
324 IS=IS-J-1
      COSG(K,3)=(Z(IS)-Z(K))/F(J+1)
325 I=K
      J=J+1
      IF (J-6) 326,330,330
330 K=I+J
      COSG(K,1)=(Z(I)-Z(K))/F(KT)
      COSG(I,2)=(Z(K)-Z(I))/F(KT)
      I=K
      J=J-1
      IF (J-JA) 330,340,332
332 IF (JA-1) 333,335,335
333 IS=IS-J
      COSG(K,3)=(Z(IS)-Z(K))/F(J)
335 COSG(K+1,3)=(Z(K)-Z(K+1))/F(J)
      COSG(K,4)=(Z(K+1)-Z(K))/F(J)
      GO TO 330
340 COSG(K,4)=(2.0*J-Z(K))/F(J)
      COSG(K,2)=(2.0*(J-1)-Z(K))/F(KT)
350 COSG(IA,1)=(2.0*(JA-1)-Z(IA))/F(KT)
      COSG(IA,4)=(2.0*JA-Z(IA))/F(JA)
      JA=JA+1
      IA=IA+JA
      KT=KT-1
      IF (KT-1) 370,370,310
370 COSG(1,3)=COSG(1,4)
      COSG(21,1)=(10.0-Z(21))/F(1)
      COSG(21,2)=COSG(21,1)
      COSG(21,4)=(12.0-Z(21))/F(6)
      COSG(36,3)=COSG(36,4)
      DO 380 I=1,36
      DO 380 J=1,4
380 SING(I,J)=SQRT(1.0-COSG(I,J)**2)

```

C
C
C

4. CALCULATE MATRIX

```

      IM=1
      L=1
      M=1
410 K=6
      N=L+M-1
      DO 430 I=L,N
      DO 420 J=1,36
      AM1(IM,J)=LAZE(K)*(AX1(I,J)+AX2(I,J))
      AM1(IM,J+36)=SINT*AM1(IM,J)

```

```

      AM1(IM,J+72)=-((EA-H/SING(I,1))*COSG(I,1)/F(K)*AX1(I,J)
1      +(EA-H/SING(I,2))*COSG(I,2)/F(K)*AX2(I,J)
      AM1(IM+1,J)=AM1(IM,J+36)
      AM1(IM+1,J+36)=(H*COST**2/SING(I,1)+EA*SINT**2)/F(K)*AX1(I,J)
1      +(H*COST**2/SING(I,2)+EA*SINT**2)/F(K)*AX2(I,J)
      AM1(IM+1,J+72)=SINT*AM1(IM,J+72)
      AM1(IM+2,J)=AM1(IM,J+72)
      AM1(IM+2,J+36)=AM1(IM+1,J+72)
      AM1(IM+2,J+72)=(H*SING(I,1)+EA*COSG(I,1)**2)/F(K)*AX1(I,J)+(H*SING
1(I,2)+EA*COSG(I,2)**2)/F(K)*AX2(I,J)
420 CONTINUE
      IM=IM+3
430 K=K-1
      L=N+1
      M=M+1
      IF (L-21) 410,440,440
440 M=M-2
      IF (L-36) 410,410,440
445 IM=1
      K=1
      L=1
450 N=L+K-1
      DO 465 I=L,N
      DO 460 J=1,36
      AM2(IM,J)=(H*COST**2/SING(I,3)+EA*SINT**2)/F(K)*AX3(I,J)+(H*COST**
12/SING(I,4)+EA*SINT**2)/F(K)*AX4(I,J)
      AM2(IM,J+36)=EA*SINT/F(K)*(AX3(I,J)+AX4(I,J))
      AM2(IM,J+72)=+(EA-H/SING(I,4))*SINT*COSG(I,4)/F(K)*AX4(I,J)
      AM2(IM+1,J)=AM2(IM,J+36)
      AM2(IM+1,J+36)=EA/F(K)*(AX3(I,J)+AX4(I,J))
      AM2(IM+1,J+72)=(EA-H/SING(I,4))*COSG(I,4)/F(K)*AX4(I,J)
      AM2(IM+2,J+36)=AM2(IM+1,J+72) -(EA-H/SING(I,3))*COSG(I,3)/F(K)
1      *AX3(I,J)
      AM2(IM+2,J)=AM2(IM,J+72) -(EA-H/SING(I,3))*SINT*COSG(I,3)/F(K)
1      *AX3(I,J)
      AM2(IM+2,J+72)=(H*SING(I,4)+EA*COSG(I,4)**2)/F(K)*AX4(I,J)
      IF (I-J) 452,455,452
452 AX3B(I,J)=ABS(AX3(I,J))
      GO TO 456
455 AX3B(I,J)=AX3(I,J)
456 AMX(IM,J+72)=-((EA-H/SING(I,3))*SINT*COSG(I,3)/F(K)*AX3B(I,J)
      AMX(IM+1,J+72)=-((EA-H/SING(I,3))*COSG(I,3)/F(K)*AX3B(I,J)
      AMX(IM+2,J+72)=(H*SING(I,3)+EA*COSG(I,3)**2)/F(K)*AX3B(I,J)
460 CONTINUE
465 IM=IM+3
      L=L+K
      K=K+1
      IF (L-21) 450,450,470
470 K=K-2
      IF (L-36) 450,450,470
475 DO 490 I=1,108
      S(I)=S1(I)
      DO 480 J=1,72
480 AMX(I,J)=AM1(I,J)+AM2(I,J)
      DO 482 J=73,108
482 AMX(I,J)=AM1(I,J)+AM2(I,J)+AMX(I,J)
490 CONTINUE
C
C 5. SOLVE FOR DISPLACEMENTS,TEST FOR CONVERGENCE AND RECALCULATE
C
      NK=108

```

```

CALL SINC(AMX,B,NR,KS)
DO 510 I=1,108
DIS(I)=DIS(I)+B(I)
510 B(I)=LD*B(I)
DO 515 I=1,36
515 Z(I)=Z1(I)+DIS(I+72)
KH=KH+1
IF (KH-LD) 300,550,550
550 LDN=LD/10
PRINT 160,LDN,(B(I),I=1,108)
DO 560 I=1,108
560 B(I)=DIS(I)
PRINT 525,KS,LD,KH
PRINT 520,KH
520 FORMAT (13HINCREMENT NO,13/59HJOINT NO      EPSI DISPL      ETA
11SPL      Z DISPL      )
525 FORMAT (1HC,3I2)
DO 540 IX=1,36
PRINT 530,IX,(B(I),I=IX,108,36)
530 FORMAT (1HC,15,5X,3E16.8)
540 CONTINUE
C
C 6. CALCULATE TENSION INCREMENTS
C
KT=6
IA=1
JA=1
IS=37
610 I=IA
J=JA
620 K=I+J
DELT(K,1)=EA/E(KT)*(-A/E(KT)*(B(I)-B(K))-A*SINT/F(KT)*(B(I+36)
1-B(K+36))+COSG(K,1)*(B(I+72)-B(K+72)))
DELT(K+1,3)=EA/E(J+1)*(-A*SINT/F(J+1)*(B(K)-B(K+1))-A/E(J+1)
1*(B(K+36)-B(K+37))+COSG(K+1,3)*(B(K+72)-B(K+73)))
IF (JA-1) 625,624,625
624 IS=IS-J-1
DELT(K,3)=EA/E(J+1)*(+A*SINT/F(J+1)*(B(IS)+B(K))+A/E(J+1)*(B(IS+3
1)+B(K+36))+COSG(K,3)*(B(IS+72)-B(K+72)))
625 I=K
J=J+1
IF (J-6) 627,630,630
630 K=I+J
DELT(K,1)=EA/E(KT)*(-A/E(KT)*(B(I)-B(K))-A*SINT/F(KT)*(B(I+36)
1-B(K+36))+COSG(K,1)*(B(I+72)-B(K+72)))
I=K
J=J-1
IF (J-JA) 630,640,632
632 IF (JA-1) 633,633,635
633 IS=IS-J
DELT(K,3)=EA/F(J)*(+A*SINT/F(J)*(B(IS)+B(K))+A/F(J)*(B(IS+36)
1+B(K+36))+COSG(K,3)*(B(IS+72)-B(K+72)))
635 DELT(K+1,3)=EA/F(J)*(-A*SINT*(B(K)-B(K+1))/F(J)-A/F(J)*(B(K+36)
1-B(K+37))+COSG(K+1,3)*(B(K+72)-B(K+73)))
GO TO 630
640 DELT(K,4)=EA/E(J)*(-A*SINT/F(J)*B(K)-A/E(J)*B(K+36)-COSG(K,4)*
1B(K+72))
DELT(K,2)=EA/E(KT)*(-A/E(KT)*B(K)-A*SINT/F(KT)*B(K+36)
1-COSG(K,2)*B(K+72))
650 DELT(IA,1)=EA/E(KT)*(A/E(KT)*B(IA)+A*SINT/F(KT)*B(IA+36)
1-COSG(IA,1)*B(IA+72))

```



```

DELT(IA,4)=EA/F(JA)*(-A*SINT/F(JA)*L(IA)-A/F(JA)*B(IA+36)
1=COSG(IA,4)*C(IA+ZL))
JA=JA+1
IA=IA+JA
KT=KT-1
IF (KT-1) 670,670,610
670 DELT(1,3)=DELT(36,4)
DELT(21,1)=EA/F(1)*(A/F(1)*B(21)+A*SINT/F(1)*B(57)
1-COSG(21,1)*B(93))
DELT(21,2)=EA/F(1)*(-A/F(1)*B(21)-A*SINT/F(1)*B(57)
1-COSG(21,2)*B(93))
DELT(21,4)=EA/F(6)*(-A*SINT/F(6)*B(21)-A/F(6)*B(57)
1-COSG(21,4)*B(93))
DELT(36,3)=DELT(1,4)
PRINT 675
675 FORMAT (26H SECTION TENSION INCREMENT SECTION TENSION INCREMENT SECTI
IN TENSION INCREMENT SECTION TENSION INCREMENT)
DO 685 IX1=1,18
IX2=IX1+18
IX3=IX2+18
IX4=IX3+18
PRINT 680,IX1,DELT(IX1,1),IX2,DELT(IX2,1),IX3,
1DELT(IX1,3),IX4,DELT(IX2,3)
680 FORMAT (1H0, 18,2X,E16.8,16,2X,E16.8,16,2X,E16.8,16,2X,E16.8)
685 CONTINUE
JP=0
JP=1
690 JP=JP+JP
IX4=IX4+1
PRINT 691,IX4,DELT(IP,4)
691 FORMAT (1H0,71X,16,2X,E16.8)
JP=JP+1
IF (IP-21) 690,692,692
692 IX4=IX4+1
JP=JP-2
PRINT 693,IX4,DELT(IP,2)
693 FORMAT (1H0,71X,16,2X,E16.8)
IF (IP-36) 690,695,695
695 IF (LD-10) 240,309,698
698 IF (LD-90) 240,699,699
699 KLD=KLD+1
IF (KLD-2) 200,700,700
700 CONTINUE
STOP
END

```

//GO.SYSIN DD *

Bibliography

1. Esquillan, N. and Saillard, Y., eds. Hanging Roofs: Proceedings of the IASS Colloquium on Hanging Roofs Continuous Metallic Shell Roofs and Superficial Lattice Roofs held in Paris, 9-11 July 1962. Amsterdam: North-Holland Publishing Co, 1963.
2. Siev, A. and Eidelman, J. Shapes of Suspended Roofs, Hanging Roofs. Amsterdam: North-Holland Publishing Co., 1963. Pp42-47.
3. Siev, A. and Eidelman, J. Stress Analysis of Prestressed Suspended Roofs, Proceedings of the ASCE, Journal of the Structural Division, August 1964, 103-121.
4. Siev, A. A General Analysis of Prestressed Nets, International Association for Bridge and Structural Engineering- Publications, 1963, 283-292.
5. Thornton, C.H. and Birnstiel, C. Three Dimensional Suspension Structures, Proceedings of the ASCE, Journal of the Structural Division, April 1967, 247-270.
6. Krishna, P. and Sparkes, S. R. An Influence Coefficient Method for Pretensioned Cable Systems, Proceedings of the Institution of Civil Engineers, London, Nov. 1968, 543-548.
7. Buchholdt, H. A. Deformation of Prestressed Cable-nets, Civil Engineering and Building Construction Series No. 38, Trondheim, 1966, 16 pp.
8. Bathish, G. N. Membrane Analysis of Cable Roofs. Ph.D. Thesis, University of Pennsylvania, 1966.
9. Siev, A. Prestressed Suspended Roofs Bounded by Main Cables, International Association for Bridge and Structural Engineering-Publications, 1967, 171-185.
10. Siev, A. Stability of Prestressed Suspended Roofs, D.Sc. Thesis, Technion-Israel Institute of Technology, 1961.

VITA AUCTORIS

- 1939 Born September 29 in Jaffna, Ceylon.
- 1960 Entered the University of Ceylon.
- 1964 Graduated with Bachelor in Science of Engineering (Honours) degree from the University of Ceylon. Joined the Faculty of Engineering, University of Ceylon as an instructor.
- 1965 Joined the Public Works Department of the Government of Ceylon as an assistant Engineer.
- 1967 Awarded Commonwealth Scholarship by the Government of Canada for graduate study at the University of Windsor.
- 1968 Elected member of the Institution of Civil Engineers, London.